N62-13944

NASA TN D-1288

NASA TN D-1288

TECHNICAL NOTE

D-1288

ANALYTICAL INVESTIGATION OF PERFORMANCE OF TWO-STAGE TURBINE OVER A RANGE OF RATIOS OF SPECIFIC HEATS FROM 1.2 TO $1\frac{2}{3}$

By Warren J. Whitney and Warner L. Stewart

Lewis Research Center
Cleveland, Ohio

NATIONAL AERONAUTICS AND SPACE ADMINISTRATION

WASHINGTON July 1962

NATIONAL AERONAUTICS AND SPACE ADMINISTRATION

TECHNICAL NOTE D-1288

ANALYTICAL INVESTIGATION OF PERFORMANCE OF TWO-STAGE TURBINE OVER A RANGE OF RATIOS OF SPECIFIC HEATS FROM 1.2 TO $1\frac{2}{3}$

By Warren J. Whitney and Warner L. Stewart

SUMMARY

The effect of the specific-heat ratio γ on overall turbine performance was investigated analytically. The turbine model used in the analysis was a two-stage impulse turbine designed for a research investigation in a sodium-vapor facility. Turbine-performance characteristics were obtained for γ-values of 1.2, 1.4, 1.53, and $1\frac{2}{3}$. A performance map was obtained at each γ-value covering a range of pressure ratios for speeds of 40, 60, 80, 100, and 120 percent of design speed.

The results of the anlysis indicated primarily that overall performance was only slightly affected by the variation of γ. A secondary effect was noted, however, in that as γ increased the velocities in the second-stage rotor increased and caused the turbine design point to lie closer to the limiting-loading point at the higher values of γ. This secondary effect caused the design-point efficiency to drop from 0.745 for γ-values of 1.2, 1.4, and 1.53 to 0.730 for a γ-value of $1\frac{2}{3}$. It was concluded from the results that in most cases the equivalence parameters (blade- to jet-speed ratio and ratio of blade speed to inlet critical velocity) would be adequate to correct from one operating fluid to another. In cases such as those encountered herein, however, in which the design point approaches the limiting loading condition, a better blade-speed parameter was shown to be the ratio of blade speed to the average of the critical velocity at the turbine inlet and the outlet.

INTRODUCTION

The problem of obtaining reliable experimental performance results of turbines under actual operating conditions is in many cases severely complicated because the properties of the working fluid are not known to a satisfactory degree of accuracy, and the accuracy and reliability of the instrumentation are inadequate. In such instances it is advantageous to obtain an aerodynamic evaluation of the turbine with a test fluid, the properties of which are well known, such as nitrogen or air, and with test conditions such that accurate performance measurements can be easily made. Tests of turbines designed for hydrogen-fueled turbopump applications, for example, were made at the Lewis Research Center with both nitrogen and hydrogen (refs. 1 and 2) and showed that testing such units with nitrogen yields an accurate description of the turbine performance with hydrogen. One reason why this agreement might be expected from these two fluids of different properties is that the ratio of specific heat at constant pressure to that at constant volume γ is practically the same for both fluids. There are, however, applications in which the real fluid has a γ-value considerably different from that of the test fluid. Monatomic gases, for example, have a γ-value of $1\frac{2}{3}$, while gases generated fuel rich from hydrocarbon fuels have values of γ of the order of 1.2. It was therefore of interest to determine analytically if turbine performance was significantly affected by a variation in the value of γ.

Accordingly, an analytical investigation was made to determine the effect of γ on overall turbine performance of a given turbine. The turbine model used was a two-stage impulse turbine that was designed for a research program in a sodium-vapor facility. Analytical performance results that were obtained assumed a perfect gas with γ-values of 1.2, 1.4, 1.53, and $1\frac{2}{3}$. Performance characteristics were obtained for speeds corresponding to 40, 60, 80, 100, and 120 percent of design speed for each value of γ, and the pressure ratio was varied over a wide range for each speed.

The results of the analytical investigation are presented herein. Included is a description of the turbine design features required for the analysis and a development of the method used. The results include both overall performance and internal-flow conditions as indicated by the resultant velocity diagrams obtained at design speed and design blade- to jet-speed ratio for the four γ-values considered.

DESCRIPTION OF TURBINE MODEL

The turbine model used in the analysis was a two-stage impulse turbine designed to operate in a sodium-vapor facility. The design inlet temperature was 2060° R. From the mean-section design-velocity diagram shown in figure 1, the following features can be noted:

(1) The turning in the blade row is 70° and 66.4° in the stators and 104.9° and 93.4° in the rotors for the first and second stages, respectively.

(2) The diagrams for the two stages are similar in that both have a stage speed-work parameter λ of 0.5, equal work extraction, and an axial direction for the outlet velocity. (All symbols are defined in appendix A).

The annular area variation through the turbine is shown in figure 2. The mean radius is constant and the area changes between stations 2 and 3. The area at stations 3 and 4 is 1.67 of that at stations 0, 1, and 2. The turbine blading geometry used as a model for the analysis is also shown in figure 2. For simplicity, the blades in the analysis were assumed to have zero trailing-edge thicknesses and straight suction surfaces downstream of the throats. The result of this assumption was that the blade-outlet angle and the free-stream flow angle were equal for all flow conditions except supercritical. The blade inlet angles were assumed to be oriented to the free-stream velocity-diagram flow angle.

In addition to the velocity diagram and geometric features of the turbine model, two equivalence parameters are needed, namely, the blade-speed parameter $U/V_{cr,0}$ and the blade- to jet-speed ratio ν. Values of γ and R for the sodium turbine were estimated as 1.53 and 57.6, respectively. The parameter $U/V_{cr,0}$ could then be calculated since U, T_0, γ, and R were known. The blade- to jet-speed ratio can be determined from the velocity diagram if the efficiency is known, since the ideal jet velocity V_j is related to the ideal enthalpy change based on total- to static-pressure ratio across the turbine. The efficiency for the velocity diagram was estimated to be 0.725 by using reference 3 as a guide. The design values of $U/V_{cr,0}$ and ν that were determined for the turbine model and were used in the analysis were 0.4587 and 0.301, respectively. The design velocity diagram, blading geometry, design efficiency, and design-point values of $U/V_{cr,0}$ and ν thus comprise the information required to proceed with the analysis.

METHOD OF ANALYSIS

The method of analysis was similar to that of reference 4 in that the procedure involved a step-by-step solution of flow conditions from station to station, which started at the turbine inlet and proceeded along the flow path. The two independent variables assumed for any calculated performance point were rotor speed $U/V_{cr,0}$ and for each rotor speed, a range of first-stage-stator-outlet critical-velocity ratios $(V/V_{cr})_1$ (or $V_1/V_{cr,0}$ since $V_{cr,1} = V_{cr,0}$). The level of stator-outlet critical-velocity ratio ultimately determines the turbine overall pressure ratio for all cases in which no blade row is choked.

The prime loss determinant was a kinetic energy loss coefficient k (see ref. 3). This method of loss determination assumes, in effect, that the loss is proportional to the average kinetic energy in the blade row, which in this analysis was based on the free-stream velocity into and out of the blade row. The other assumption used in the performance calculations was that the component of velocity normal to the blade-inlet direction of any given blade row did not contribute to the dynamic pressure head, and thus a loss in total pressure across the blade row was effected.

The value of k was determined, as described in appendix B, from the design velocity diagram (fig. 1) and the efficiency - speed-work-parameter curve of reference 3. This value of k was then used for all calculated performance points over the entire range of speeds, pressure ratios, and γ-values. A detailed description of the method and the equations used is given in appendix C.

RESULTS OF ANALYSIS

The analysis of the turbine was made for γ-values of 1.2, 1.4, 1.53, and $1\frac{2}{3}$. Although the results include design and off-design performance, the discussion will be principally concerned with design performance. The off-design performance is important in that it can be used to discern the trends of efficiency with speed or efficiency with pressure ratio that occur in the design-point region and thereby it can facilitate an understanding of the behavior of design-point performance over the range of γ-values. The results of the analysis will be presented as follows: First, the results for a γ of 1.53 will be presented as those most closely representing the γ-value for which the model turbine was designed. These results will then be compared with those obtained at a γ of 1.4, which represents the air test. Finally, the results obtained at the extreme values of 1.2 and $1\frac{2}{3}$ will be presented and, together with those previously described, will be used to demonstrate the effects of such a wide variation of γ on the turbine performance and internal flow conditions.

Performance at Ratio of Specific Heats of 1.53

The performance of the turbine obtained at a γ of 1.53 is presented in figure 3, in which the equivalent specific work and weight-flow characteristics are shown as functions of the turbine total- to static-pressure ratio for 40, 60, 80, 100, and 120 percent of design speed. The work is shown corrected to reference inlet conditions (NACA standard air). The design value of $\Delta h'/\theta_{cr}$ was determined from the velocity diagram (fig. 1), inlet temperature, and estimated values of γ and R to be 34.9 Btu per pound for the sodium turbine model. At design speed and design pressure ratio (6.85), the equivalent specific work of 35.7 Btu per pound that was obtained (fig. 3(a)) compared favorably with the design value. Also, the design point was close to limiting loading, as maximum work was 1.05 of design work. As mentioned in the DESCRIPTION OF TURBINE MODEL, the two parameters that define the design point were $U/V_{cr,0}$ and ν. The design value of pressure ratio was determined from the design values of $U/V_{cr,0}$ and ν for any value of γ by use of equation (1).

$$\nu = \frac{\dfrac{U}{V_{cr,0}}}{\left\{\dfrac{\gamma + 1}{\gamma - 1}\left[1 - \left(\dfrac{p_4}{p_0'}\right)^{\frac{\gamma-1}{\gamma}}\right]\right\}^{1/2}} \tag{1}$$

The turbine weight-flow characteristics are presented in figure 3(b) with the weight flow, which was normalized by the first-stage-stator ideal critical weight flow, shown as a function of total- to static-pressure ratio. The first-stage stator was choked for all speeds at a pressure ratio of about 3, which is considerably below the design pressure ratio. The value of the choking weight-flow ratio indicates that a flow coefficient of 0.935 was obtained in the analysis. The weight-flow trends shown are typical of those obtained over the range of γ-values considered with the first-stage stator choked at pressure ratios considerably below design. The flow coefficient varied from about 0.95 at a γ of 1.2 to 0.93 at a γ of $1\frac{2}{3}$.

The turbine efficiency is shown in figure 4 as a function of blade- to jet-speed ratio ν for the various speeds investigated. At design ν (0.301) and speed, a static efficiency of 0.745 was obtained. The fact that this point lay on a portion of the design-speed curve where efficiency was rapidly decreasing with decreasing blade- to jet-speed ratio is characteristic of a turbine operating near limiting loading.

The velocity diagram obtained at design speed and pressure ratio is presented in figure 5. A comparison with the turbine-model diagram of figure 1 shows that only minor deviations occurred. Incidence angles of 2° or less were encountered with a negligible effect on efficiency. The outlet critical-velocity ratio (0.646) also indicates that the design point was close to the limiting-loading work for this value of γ.

Performance at Ratio of Specific Heats of 1.4

The performance results obtained for a γ of 1.4 are shown in figures 6 to 8. The equivalent specific work is shown in figure 6 as a function of pressure ratio. At design speed and pressure ratio (5.55 as calculated by eq. (1)), an equivalent specific work of 35.8 Btu per pound was obtained, which was close to the 35.7 value obtained at a γ of 1.53. The trends of the specific-work curves are similar to those obtained for a γ of 1.53 (fig. 6); however, at the design point, the margin with respect to limiting loading had so increased that limiting-loading work was 1.10 that of design.

The efficiency characteristics at a γ of 1.4 are presented in figure 7 in a manner similar to that of figure 4. At design speed and ν, an efficiency of 0.745 was obtained, which was the same as that obtained at a γ of 1.53. A comparison of the position of the design point on the design-speed curve with that of figure 4 shows that the design point moved closer to the peak of the efficiency curve as a result of reducing γ from 1.53 to 1.4.

The design-point velocity diagram obtained at a γ of 1.4 is presented in figure 8. The diagram was comparable with that obtained at a γ of 1.53; the incidence angles of the rotors were less than $\pm 1.5^{\circ}$ and that of the second-stage stator was 3.2°. Little effect on efficiency would again be expected. The one significant change was at the turbine outlet, where the critical-velocity ratio was reduced from 0.646 to 0.532. Such a reduction was another indication that the design point was further removed from limiting loading as a result of reducing γ from 1.53 to 1.4. Also to be noted as a result of the reduction in second-stage-rotor-outlet relative velocity (0.868 to 0.730) is that the turbine-outlet flow angle changed from -5.4° to $+1.9^{\circ}$ with little effect on performance.

Performance at Ratio of Specific Heats of 1.2

The results of the analysis made for a γ of 1.2 are presented in figures 9 to 11. The specific-work characteristics presented in figure 9 show that at design pressure ratio (4.15) and speed an equivalent specific work of 35.8 Btu per pound was obtained. This value was nearly the same as that obtained at γ-values of 1.4 and 1.53. The margin between limiting-loading and design-point work was increased considerably; limiting-loading work was 1.21 that of the design-point work. The 40-percent-design-speed results are not shown in figure 9 because they were below the scale of the curve; the highest equivalent specific work obtained was 16.12 Btu per pound. At design ν an efficiency of 0.745 was again obtained with the design point near peak efficiency (fig. 10). The design-point velocity diagram in figure 11 shows that the critical-velocity ratio at the exit was reduced to 0.452. Rotor incidence angles were again low. The second-stage-stator incidence angle was 5.3°. The effect on performance was small, however, because of the low associated velocity. Little change in overall performance or internal-flow conditions was experienced at this γ because the turbine design-point operation was more conservative with respect to limiting loading.

Performance at Ratio of Specific Heats of $1\frac{2}{3}$

Figures 12 to 14 present the results of the analysis obtained at a γ of $1\frac{2}{3}$. In this case, an equivalent specific work of 35.1 Btu per pound, which was 2 percent below the value obtained for a γ of 1.53, was obtained at design pressure ratio (8.78) and design speed (fig. 12). Furthermore, the limiting-loading specific work was only 1.01 that of the design point. The efficiency at the design point was 0.730 (fig. 13) with the design point on a portion of the design-speed curve where efficiency decreased sharply with decreasing blade- to jet-speed ratio. The increase of the second-stage rotor incidence to 3.4° had some small effect on the efficiency for the level of velocity at this station (fig. 14). Also, the outlet critical-velocity ratio was increased to 0.743, which corresponded to turbine operation near limiting loading. From these results, it is evident that, as the value of γ is increased to $1\frac{2}{3}$, the turbine design point will fall close to limiting-loading work with an alteration in the turbine-outlet diagram and a subsequent reduction in efficiency.

Off-Design Performance

As mentioned previously, the discussion of the analytical results has been primarily concerned with design-point performance. The off-design performance is included, however, and may be of interest in certain instances. The performance results were correlated by blade- to jet-speed ratio over the range of conditions except for the depressed efficiencies that occurred near limiting loading (see figs. 4, 7, 10 and 13). Plotting the envelopes of the efficiencies from figures 4, 7, 10, and 13 on one curve showed that the agreement of the envelope efficiencies was within approximately 1 point if the dropoff in efficiency near the limiting-loading point were ignored. The effect of γ on off-design performance can be concluded to be small except for the case in which the turbine is operating near limiting loading.

DISCUSSION

The results of the analyses showed that for the turbine under study, the effect of γ on performance was, in general, very small; however, in the case of a γ of $1\frac{2}{3}$, a reduction in design-point efficiency of 1.5 points was noted. Also, this reduction in efficiency evidently resulted from the proximity of the turbine design point to limiting loading, since the design-point work was 1.5 percent below the limiting-loading work. The velocity diagrams in figures 5, 8, 11, and 14 show that although $U/V_{cr,0}$ (or $U/V_{cr,1}$ since $U/V_{cr,0} = U/V_{cr,1}$) was constant at the specified design value, $U/V_{cr,4}$ changed substantially and varied from 0.499 at a γ of 1.2 to 0.604 at a γ of $1\frac{2}{3}$. From this variation it is indicated that, although Mach number conditions were similar at the inlet, they changed considerably at the outlet. This trend suggests that a better correlation of results might be obtained if the blade-speed parameter were based on a critical velocity at the turbine outlet. Specifying constant ν and $U/V_{cr,4}$ would, in turn, specify that the turbine design point retain the same relation to limiting loading over the range of γ-values. This specification causes the turbine correlating points to be at off-design speeds when based on $U/V_{cr,0}$. The ratio of $U/V_{cr,0}$ to $U/V_{cr,4}$ is a function of the total-temperature ratio across the turbine as follows:

$$\frac{\left(\frac{U}{V_{cr,0}}\right)^2}{\left(\frac{U}{V_{cr,4}}\right)^2} = \frac{T_4'}{T_0'} = \frac{T_4'}{T_4' + \Delta T'} = \frac{1}{1 + \frac{\Delta T'}{T_4'}} \tag{2}$$

Now

$$\Delta T' = \eta_s \, \Delta T_{id}$$

Introducing equation (2) and substituting into equation (1) yield, when rearranged,

$$\frac{U}{V_{cr,0}} = \frac{\dfrac{U}{V_{cr,4}}}{\left[1 + \eta_s\left(\dfrac{\gamma - 1}{\gamma + 1}\right)\left(\dfrac{\dfrac{U}{V_{cr,4}}}{\nu}\right)^2\right]^{1/2}} \tag{3}$$

New values of $U/V_{cr,0}$ were calculated with equation (3) for γ-values of 1.2, 1.4, and $1\frac{2}{3}$ by using a γ of 1.53 as a base point (with $(U/V_{cr})_4 = 0.5730$ thereby specified) and by retaining the design value of ν (0.301). The efficiency value must be estimated and an iterative procedure must be used to solve equation (3). The efficiencies at the off-design speeds were obtained from cross plots made from figures 7, 10, and 13. The results of this calculation are presented as the dashed line in figure 15(a). The solid line represents the design value of $U/V_{cr,0}$ that was specified constant over the range of γ in the analysis. The other curve, representing a constant value of $\overline{U/V_{cr}}$, will be discussed subsequently. The dashed line in figure 15(a), representing a constant value of $U/V_{cr,4}$, shows that for γ-values below 1.53, an overspeed condition existed and at γ-values above 1.53 an underspeed condition resulted. Values of 112, 104, and 97 percent of design speed were obtained for γ-values of 1.2, 1.4, and $1\frac{2}{3}$, respectively.

The efficiencies and $U/V_{cr,0}$ values that resulted from the condition of $U/V_{cr,4} = 0.5730$ were used in equation (1) to determine the pressure ratio. These results are shown as the dashed line in figure 15(b). The solid line is included for comparison and represents the design pressure ratio for a constant $U/V_{cr,0}$. The pressure-ratio variation over the range of γ is much smaller for constant $U/V_{cr,4}$ (6.44 to 7.05). The efficiency variation is compared in figure 15(c). The dashed line in the figure shows that for a constant $U/V_{cr,4}$, the efficiency decreased at the low value of γ, probably as a result of mismatching at the inlet to the first-stage rotor. The efficiency values for the condition of a constant $U/V_{cr,4}$ were 0.712, 0.733, and 0.740 for γ-values of 1.2, 1.4, and $1\frac{2}{3}$, respectively.

From the trends of the curves of constant $U/V_{cr,0}$ and constant $U/V_{cr,4}$, specifying an average U/V_{cr} would be expected to correlate the performance results over the range of γ better than $U/V_{cr,0}$ or $U/V_{cr,4}$. This specification should so distribute the mismatching between the turbine inlet and turbine outlet that the effect of mismatching on performance at either station may not be significant. Accordingly, the following speed parameter was used:

$$\frac{\dfrac{U}{V_{cr,0}} + \dfrac{U}{V_{cr,4}}}{2} = \overline{\left(\frac{U}{V_{cr}}\right)} = \text{Constant} = 0.5158 \tag{4}$$

A γ-value of 1.53 was again used as the base point, as indicated by the constant in equation (4), and the design value of ν (0.301) was retained. Substituting equation (3) into equation (4) yields the following equation for $U/V_{cr,4}$:

$$\frac{U}{V_{cr,4}}\left\{1 + \frac{1}{\left[1 + \eta_s\left(\frac{\gamma - 1}{\gamma + 1}\right)\left(\frac{\frac{U}{V_{cr,4}}}{\nu}\right)^2\right]^{1/2}}\right\} = 0.5158 \tag{5}$$

The results of the calculations specifying a constant $\overline{U/V_{cr}}$ are shown in figure 15. On all three parts, the trend for a constant $\overline{U/V_{cr}}$ falls between the curves of constant $U/V_{cr,4}$ and $U/V_{cr,0}$. The values of design speed for constant $\overline{U/V_{cr}}$ were 107, 102, and 98 percent for γ-values of 1.2, 1.4, and $1\frac{2}{3}$, respectively. The efficiency varied from 0.734 at a γ of 1.2 to 0.745 at a γ of 1.53. The efficiency was thus correlated to approximately 1 point. It can therefore be concluded that when significant differences between inlet and outlet critical velocities exist, a blade-speed parameter based on the average of these two critical velocities should be used to correlate the results over a wide variation of γ. The use of this parameter reduces the effect of mismatching at the turbine outlet for a specified blade-inlet-speed parameter, and the effect of mismatching at the turbine inlet for a specified blade-outlet-speed parameter. Thus the effect of mismatching at either the inlet or the outlet is so reduced that this effect on overall performance is not significant.

SUMMARY OF RESULTS

An analytical investigation of the effects of varying the specific-heat ratio γ on the performance of a two-stage impulse turbine designed for a research sodium-vapor facility is presented herein. The results of the analysis can be summarized as follows:

1. At a γ of 1.53, most closely representing the γ-value for which the turbine was designed, the design-point static efficiency was 0.745. The limiting-loading work was 1.05 that of the design point and indicated the turbine to be fairly critical with respect to limiting loading. The first-stage stator was choked at a pressure ratio far below that of design.

2. As γ was reduced to 1.4, representing the air case, the efficiency of the turbine at the design point (indicated by the design value of blade- to jet-speed ratio and ratio of blade speed to inlet critical-velocity ratio) remained the same. The margin between limiting loading and design work increased, however, with a limiting-loading work 1.10 that of design, and indicated that the turbine-outlet conditions were more conservative with respect to limiting loading.

3. At the lowest value of γ investigated (1.2), the efficiency again remained constant. The limiting-loading work in this case, however, was 1.21 that of design and indicated that the turbine-outlet conditions were very conservative with respect to limiting loading.

4. For the highest value of γ investigated $(1\frac{2}{3})$, the turbine efficiency dropped to 0.730; the limiting-loading work in this case was approximately 1.01 that of design. This reduction in efficiency resulted from the proximity of the design point to limiting loading and the increased losses that accompany this condition.

5. From a comparison of the performance results correlated with three different blade-speed parameters, it was found that the performance could be correlated to approximately 1 point in efficiency over the range of γ by using the ratio of blade speed to the average of turbine-inlet and -outlet critical velocities.

CONCLUSIONS

From the results of the study, it can be concluded that except for turbines of extreme Mach number conditions, the use of constant blade- to jet-speed ratio and the ratio of blade speed to inlet critical velocity is adequate in correlating the design-point performance over a wide range of ratios of specific heats. In the cases in which the turbine design point is close to limiting loading and in which a considerable difference exists between inlet and outlet critical velocities, using a blade-speed parameter based on the average critical velocity will yield a better correlation of efficiency over a range of γ-values.

Lewis Research Center
National Aeronautics and Space Administration
Cleveland, Ohio, May 1, 1962

E-1724

APPENDIX A

SYMBOLS

g	acceleration due to gravity, 32.17 ft/sec^2
Δh	specific work, Btu/lb
i	incidence angle, deg
J	mechanical equivalent of heat, 778.2 ft-lb/Btu
k	kinetic energy loss coefficient, dimensionless
L_r	rotor energy loss, Btu/lb
L_{st}	stator energy loss, Btu/lb
l	blade length, ft
p	absolute pressure, lb/sq ft
R	gas constant, ft-lb/(lb)($^\circ$R)
r	turbine mean radius, ft
T	absolute temperature, $^\circ$R
U	mean blade speed, ft/sec
V	absolute gas velocity, ft/sec
V_j	ideal jet velocity, $\left\{2g \frac{\gamma}{\gamma - 1} RT'_0 \left[1 - \left(\frac{p_4}{p'_0}\right)^{\frac{\gamma-1}{\gamma}}\right]\right\}^{1/2}$, ft/sec
W	gas velocity relative to moving blade row, ft/sec
w	weight-flow rate, lb/sec

α absolute gas-flow angle measured from axial direction, deg

β flow angle relative to moving blade row measured from axial direction, deg

γ ratio of specific heat at constant pressure to that at constant volume

η total efficiency, based on total- to total-pressure ratio across turbine

η_s static efficiency, based on total- to static-pressure ratio across turbine

θ_{cr} squared ratio of turbine-inlet critical velocity to reference critical velocity, $(V_{cr,0}/V_{cr,ref})^2$

λ speed-work parameter, $U^2/gJ\ \Delta h'$

ν blade- to jet-speed ratio, U/V_j

ρ density, lb/cu ft

Subscripts:

cr critical velocity or flow conditions; $V_{cr} = \left(\gamma gRT' \frac{2}{\gamma + 1}\right)^{1/2}$

id ideal

ref reference state; $V_{cr,ref} = 1019.4$ ft/sec

u tangential component

x axial component

0 turbine inlet (see fig. 2)

1 station at first-stage-stator outlet (first-stage-rotor inlet)

2 station at first-stage-rotor outlet (second-stage-stator inlet)

3 station at second-stage-stator outlet

4 station at turbine outlet

E-1524

Superscripts:

' absolute total state

" total state relative to moving blade row

APPENDIX B

DETERMINATION OF KINETIC ENERGY LOSS COEFFICIENT

As mentioned in the METHOD OF ANALYSIS, the primary loss determinant was the kinetic energy loss coefficient k. The value of k was determined from the design velocity diagrams and the design predicted efficiency as follows:

$$\eta = \frac{\Delta h'}{\Delta h' + \sum L_{st} + \sum L_r}$$

The work term $\Delta h'$ can be expressed in terms of velocity-diagram quantities as

$$\Delta h' = \frac{U}{gJ}\left[\left(V_{u,1} - V_{u,2}\right) + \left(V_{u,3} - V_{u,4}\right)\right], \text{ Btu/lb}$$

The loss terms L_{st} and L_r can be expressed typically as

$$L_{st,0-1} = \frac{k}{2gJ}\left(V_0^2 + V_1^2\right), \text{ Btu/lb}$$

and

$$L_{r,1-2} = \frac{2k}{2gJ}\left(W_1^2 + W_2^2\right), \text{ Btu/lb}$$

for the first-stage stator and rotor, respectively. The factor 2 was used in the rotor loss terms for reasons discussed in reference 3.

The efficiency η was 0.80, as determined from the velocity diagram of figure 1 by using the efficiency - speed-work-parameter curve of reference 3 as a guide. Thus, since the efficiency and the velocity diagram are known, the value of k can be determined. The value of k determined for this study was 0.082889.

The static efficiency η_s was determined similarly except that the equation was changed to include the residual leaving energy.

$$\eta_s = \frac{\Delta h'}{\Delta h' + \sum L_{st} + \sum L_r + \frac{V_4^2}{2gJ}}$$

The static efficiency was 0.725.

As in reference 3, this type of efficiency determination ignores the effect of reheat in a multistage turbine. The actual overall efficiency as calculated by the analysis would be expected to be slightly higher because of the reheat effect.

APPENDIX C

ANALYTICAL PROCEDURE

The analytical procedure involved a step-by-step solution of flow conditions through the turbine, as mentioned in the METHOD OF ANALYSIS. The two variables that were fixed for any given calculation point were first-stage-stator-outlet velocity $(V/V_{cr})_1$, and blade speed $U/V_{cr,1}$. The representative velocity diagram and flow conditions were taken to be those at the mean radius. The blade length changed in the second-stage stator and the actual annular area variation had to be considered in the continuity relations.

The calculations were made for five values of $U/V_{cr,1}$ corresponding to 40, 60, 80, 100, and 120 percent of design speed. For each speed a range of $(V/V_{cr})_1$ was assumed. The blade-outlet flow angles used were the free-stream flow angles, as indicated on the velocity diagram. The flow was assumed to conform to this angle for values of $(V/V_{cr})_1$ of 1.0 or lower. For values of $(V/V_{cr})_1$ exceeding 1.0, the flow was assumed to deflect toward the axial direction to maintain continuity. The values of V/V_{cr} and W/W_{cr} were arbitrarily limited to 1.25 at the exit of all blade rows except the second-stage rotor, because the shock losses would become appreciable in this range of Mach number. This limit of $(V/V_{cr})_1$ of 1.25 limited the overall pressure ratio at a γ-value of 1.2 and 40 percent design speed. At no other condition did a blade-outlet critical-velocity ratio attain this value, because of choking at a downstream station. The value of W/W_{cr} out of the second-stage rotor was allowed to increase until limiting loading occurred for this blade row.

The sequence of the procedure was as follows: Values of $(V/V_{cr})_1$ were assumed for any given speed with a starting value of 0.4 and with increasing increments of 0.05 to the arbitrary limit of 1.25 or until a blade row choked downstream. When a blade row choked, an iteration was required to determine accurately the corresponding value of $(V/V_{cr})_1$. Conditions upstream of the choking point were then held fixed, and the V/V_{cr} or W/W_{cr} out of the choking blade row was allowed to increase to the limit of 1.25 or until another blade row choked downstream of the choking row.

The calculation procedure and equations used are outlined in the following paragraphs. From consideration of the energy equation, the total temperature and critical velocity remain constant across any given blade row.

First-stage stator. - The two quantities that must be evaluated for this blade row are total-pressure ratio p_1'/p_0' and mass flow $(\rho V/\rho' V_{cr})_1$. The value of $(V/V_{cr})_1$ is assumed as an independent variable. Equations (C1) and (C2) are isentropic relations between total and static conditions.

$$\left(\frac{\rho V}{\rho' V_{cr}}\right)_1 = \left[1 - \frac{\gamma - 1}{\gamma + 1}\left(\frac{V}{V_{cr}}\right)_1^2\right]^{\frac{1}{\gamma - 1}}\left(\frac{V}{V_{cr}}\right)_1 \tag{C1}$$

$$\left(\frac{p}{p'}\right)_1 = \left[1 - \frac{\gamma - 1}{\gamma + 1}\left(\frac{V}{V_{cr}}\right)_1^2\right]^{\frac{\gamma}{\gamma - 1}} \tag{C2}$$

The equation for loss pressure ratio across a blade row was evolved from two basic concepts. The first, as mentioned in the METHOD OF ANALYSIS, was that the loss is proportional to the average kinetic energy in the blade row, expressed algebraically as

$$L_{st,0-1} = \frac{k}{2gJ}\left(V_0^2 + V_1^2\right)$$

If there were an incidence angle to consider at station 0, the loss would be modified as

$$L_{st,0-1} = \frac{k}{2gJ}\left(V_0^2 + V_1^2\right) + \frac{\sin^2 i_0}{2gJ} V_0^2$$

The second basic concept was that the loss in kinetic energy is reflected as the difference between the actual outlet velocity and the ideal outlet velocity, expressed algebraically as follows:

$$V_{1,id}^2 - V_1^2 = k\left(V_0^2 + V_1^2\right) + \sin^2 i_0 \, V_0^2$$

The pressure-loss equations were developed similarly for all blade rows by use of these two considerations. For the first-stage stator the loss equation in nondimensional form is as follows:

$$\frac{p_1'}{p_0'} = \left\{1 - \frac{\frac{\gamma - 1}{\gamma + 1} k \left[\left(\frac{V}{V_{cr}}\right)_0^2 + \left(\frac{V}{V_{cr}}\right)_1^2\right]}{1 - \frac{\gamma - 1}{\gamma + 1}\left(\frac{V}{V_{cr}}\right)_1^2}\right\}^{\frac{\gamma}{\gamma-1}} \tag{C3}$$

In the solution of these equations an iterative procedure must be used since $(V/V_{cr})_0$ is not known for the assumed value of $(V/V_{cr})_1$. The continuity relation must be maintained such that

$$\left(\frac{\rho V}{\rho' V_{cr}}\right)_1 \cos \alpha_1 = \left(\frac{\rho V}{\rho' V_{cr}}\right)_0 \frac{p_0'}{p_1'} \tag{C4}$$

Equation (C1) can be applied at station 0 to obtain the relation between the mass-flow parameter $(\rho V/\rho' V_{cr})_0$ and critical-velocity ratio $(V/V_{cr})_0$.

For values of $(V/V_{cr})_1$ exceeding 1, it was assumed that the flow rate was constant and equal to that at $(V/V_{cr})_1 = 1.0$ and that the flow angle was the particular angle required to maintain continuity for the given expansion ratio and the calculated pressure loss. This procedure was used for all blade rows for supercritical expansion ratios.

<u>First-stage rotor</u>. - The inlet total state of the first-stage rotor is determined from the total-state conditions out of the first-stage stator and the isentropic total-to-static relations on a relative and absolute basis by using equations (C5) and (C6), which are as follows:

$$\left(\frac{\rho'' W_{cr}}{\rho' V_{cr}}\right)_1 = \left\{1 - \frac{\gamma - 1}{\gamma + 1}\left[\frac{2UV_{u,1}}{V_{cr,1}^2} - \left(\frac{U}{V_{cr,1}}\right)^2\right]\right\}^{\frac{\gamma+1}{2(\gamma-1)}} \tag{C5}$$

$$\left(\frac{W_{cr}}{V_{cr}}\right)_1 = \left\{1 - \frac{\gamma - 1}{\gamma + 1}\left[\frac{2UV_{u,1}}{V_{cr,1}^2} - \left(\frac{U}{V_{cr,1}}\right)^2\right]\right\}^{1/2} \tag{C6}$$

and

$$\left(\frac{W}{V_{cr}}\right)_1 = \left[\left(\frac{W_u}{V_{cr}}\right)_1^2 + \left(\frac{V_x}{V_{cr}}\right)_1^2\right]^{1/2} \tag{C7}$$

where, from the geometry of the velocity diagram,

$$\left(\frac{W_u}{V_{cr}}\right)_1 = \left(\frac{V_u}{V_{cr}}\right)_1 - \frac{U}{V_{cr,1}}$$

$$\left(\frac{V_x}{V_{cr}}\right)_1 = \left(\frac{V}{V_{cr}}\right)_1 \cos \alpha_1$$

and

$$\left(\frac{V_u}{V_{cr}}\right)_1 = \left(\frac{V}{V_{cr}}\right)_1 \sin \alpha_1$$

The outlet conditions must be determined by an iterative procedure by first assuming that $(\rho''W_{cr})_2 = (\rho''W_{cr})_1$, which in effect is assuming that $p_2'' = p_1''$.

$$\left(\frac{\rho W}{\rho''W_{cr}}\right)_2 = \left(\frac{\rho W}{\rho''W_{cr}}\right)_1 \frac{\cos \beta_1}{\cos \beta_2}$$

where the flow angle β_1 has been determined and the flow angle β_2 is the same as the blade angle, 50.9°. The value of $(W/W_{cr})_2$ is determined from the isentropic relation:

$$\left(\frac{\rho W}{\rho''W_{cr}}\right)_2 = \left[1 - \frac{\gamma - 1}{\gamma + 1}\left(\frac{W}{W_{cr}}\right)_2^2\right]^{\frac{1}{\gamma-1}}\left(\frac{W}{W_{cr}}\right)_2 \tag{C8}$$

The blade entry incidence angle is determined from the flow angle and the blade angle.

$$i_1 = 54^\circ - \beta_1$$

The component of relative velocity normal to the blade entry angle is assumed to be lost with regard to total-pressure recovery. Thus the total-pressure equation for the blade row is

$$\frac{p_2''}{p_1''} = \left(1 - \frac{\frac{\gamma - 1}{\gamma + 1}\left\{\sin^2 i_1\left(\frac{W}{W_{cr}}\right)_1^2 + 2k\left[\left(\frac{W}{W_{cr}}\right)_1^2 + \left(\frac{W}{W_{cr}}\right)_2^2\right]\right\}}{1 - \frac{\gamma - 1}{\gamma + 1}\left(\frac{W}{W_{cr}}\right)_2^2}\right)^{\frac{\gamma}{\gamma-1}} \tag{C9}$$

From the value of p_2''/p_1'' the new value of $(\rho'' W_{cr})_2$ is determined thus:

$$(\rho'' W_{cr})_2 = (\rho'' W_{cr})_1\left(\frac{p_2''}{p_1''}\right)$$

The procedure is then repeated with the new value of $(\rho'' W_{cr})_2$. The equations could then be solved for blade-outlet conditions to a very high accuracy with three to four iterations.

Second-stage stator. - The total-state conditions out of the first-stage rotor are needed since they are the inlet conditions to the second-stage stator. These quantities could also be used to evaluate the first stage as a single-stage turbine. The critical-velocity ratio across the first stage is expressed as the square root of the temperature ratio, which, in turn, was derived from the blade speed and change of momentum.

$$V_{cr,2} = V_{cr,1}\left[1 - 2\left(\frac{\gamma - 1}{\gamma + 1}\right)\left(\frac{U}{V_{cr,1}}\right)\left(\frac{\Delta V_{u,1-2}}{V_{cr,1}}\right)\right]^{1/2} \tag{C10}$$

The change in tangential velocity $\Delta V_{u,1-2}/V_{cr,1}$ is obtained from $(V_u/V_{cr})_1$ and $V_{u,2}/V_{cr,1}$, and the second quantity can be determined as follows:

$$\frac{V_{u,2}}{V_{cr,1}} = \left(\frac{W}{W_{cr}}\right)_2 \sin \beta_2 \left(\frac{W_{cr}}{V_{cr}}\right)_1 - \frac{U}{V_{cr,1}} \tag{C11}$$

The inlet pressure to the second-stage stator can be determined as follows:

$$\frac{p_2'}{p_0'} = \left(\frac{p_1'}{p_0'}\right)\left(\frac{p_1''}{p_1'}\right)\left(\frac{p_2''}{p_1''}\right)\left(\frac{p_2'}{p_2''}\right) \tag{C12}$$

Two of the four pressure ratios on the right side of the equation have been evaluated, p_1'/p_0' from equation (C3) and p_2''/p_1'' from equation (C9). The pressure ratio p_1''/p_1' can be obtained by taking the quantity in braces in equations (C5) and (C6) to the appropriate power:

$$\frac{p_1''}{p_1'} = \left\{1 - \frac{\gamma - 1}{\gamma + 1}\left[\frac{2UV_{u,1}}{V_{cr,1}^2} - \left(\frac{U}{V_{cr,1}}\right)^2\right]\right\}^{\frac{\gamma}{\gamma-1}} \tag{C13}$$

The pressure ratio p_2'/p_2'' is determined from the isentropic relations between total and static conditions on relative and absolute bases and from the tangential velocity components by use of the following equation:

$$\frac{p_2'}{p_2''} = \left[1 - \frac{\gamma - 1}{\gamma + 1}\left(\frac{W_u}{W_{cr}}\right)_2^2 + \frac{\gamma - 1}{\gamma + 1}\left(\frac{V_u}{W_{cr}}\right)_2^2\right]^{\frac{\gamma}{\gamma-1}} \tag{C14}$$

where, from the geometry of the velocity diagram,

$$\left(\frac{W_u}{W_{cr}}\right)_2 = \left(\frac{W}{W_{cr}}\right)_2 \sin \beta_2$$

and

$$\left(\frac{V_u}{W_{cr}}\right)_2 = \left(\frac{W_u}{W_{cr}}\right)_2 - \left(\frac{U}{V_{cr,1}}\right)\left(\frac{V_{cr,1}}{W_{cr,1}}\right) \qquad \text{(C15)}$$

The two components of critical-velocity ratio are then obtained:

$$\left(\frac{V_x}{V_{cr}}\right)_2 = \left(\frac{W}{W_{cr}}\right)_2 \cos \beta_2 \frac{W_{cr,2}}{V_{cr,2}} \qquad \text{(C16)}$$

$$\left(\frac{V_u}{V_{cr}}\right)_2 = \left(\frac{V_u}{W_{cr}}\right)_2 \left(\frac{W_{cr}}{V_{cr}}\right)_2 \qquad \text{(C17)}$$

where $(V_u/W_{cr})_2$ was obtained from equation (C15) and where

$$\left(\frac{W_{cr}}{V_{cr}}\right)_2 = \left(\frac{V_{cr,1}}{V_{cr,2}}\right)\left(\frac{W_{cr}}{V_{cr}}\right)_1$$

can be obtained from equations (C6) and (C10).

The incidence angle i_2 is obtained from the absolute flow angle, which is, in turn, specified by the two velocity components, and the stator blade entry angle, which was 0°.

It is assumed as a first approximation that $p_3' = p_2'$, and $(\rho V/\rho' V_{cr})_3$ can then be determined from continuity and the area ratio of stations 3 and 1 by using the following equation:

$$\left(\frac{\rho V}{\rho' V_{cr}}\right)_3 = \left(\frac{\rho V}{\rho' V_{cr}}\right)_1 \left(\frac{\cos \alpha_1}{\cos \alpha_3}\right)\left(\frac{1}{1.67}\right)\left(\frac{p_1' V_{cr,3}}{p_3' V_{cr,1}}\right) \qquad \text{(C18)}$$

By using the approximate value of $(\rho V/\rho' V_{cr})_3$, the value of $(V/V_{cr})_3$ is obtained from

$$\left(\frac{\rho V}{\rho' V_{cr}}\right)_3 = \left(\frac{V}{V_{cr}}\right)_3 \left[1 - \frac{\gamma - 1}{\gamma + 1}\left(\frac{V}{V_{cr}}\right)_3^2\right]^{\frac{1}{\gamma - 1}} \tag{C19}$$

The stator pressure ratio is then determined from

$$\frac{p_3'}{p_2'} = \left(1 - \frac{\frac{\gamma - 1}{\gamma + 1}\left\{k\left[\left(\frac{V_x}{V_{cr}}\right)_2^2 + \left(\frac{V_u}{V_{cr}}\right)_2^2 + \left(\frac{V}{V_{cr}}\right)_3^2\right] + \sin^2 i_2\left[\left(\frac{V_x}{V_{cr}}\right)_2^2 + \left(\frac{V_u}{V_{cr}}\right)_2^2\right]\right\}}{1 - \frac{\gamma - 1}{\gamma + 1}\left(\frac{V}{V_{cr}}\right)_3^2}\right)^{\frac{\gamma}{\gamma - 1}} \tag{C20}$$

The value of $(\rho V/\rho' V_{cr})_3$ from equation (C18) is corrected by dividing by p_3'/p_2', and the procedure through equations (C19) and (C20) is repeated until the assumed value of p_3'/p_2' used to enter the calculation in equation (C18) is equal to the resultant value in equation (C20). The flow angle out of the stator was assumed to be the blade angle (66.4°) for all values of $(V/V_{cr})_3$ up to 1.0. An iteration of $(V/V_{cr})_3$ is required for each speed to determine the choking point. For supercritical expansion the flow angle was allowed to deflect toward the axial direction such that

$$\left[\left(\frac{\rho V}{\rho' V_{cr}}\right)_3 \cos 66.4^\circ\right]_{(V/V_{cr})_3 = 1.0} = \left(\frac{\rho V}{\rho' V_{cr}}\right)_3 \cos \alpha_3 \frac{(\rho' V_{cr})_3}{\left[(\rho' V_{cr})_3\right]_{(V/V_{cr})_3 = 1.0}} \tag{C21}$$

Second-stage rotor. - The analytical procedure for the second-stage rotor is the same as that for the first-stage rotor. The inlet total-state conditions are determined from

$$\left(\frac{\rho'' W_{cr}}{\rho' V_{cr}}\right)_3 = \left\{1 - \frac{\gamma - 1}{\gamma + 1}\left[\frac{2UV_{u,3}}{V_{cr,3}^2} - \left(\frac{U}{V_{cr,3}}\right)^2\right]\right\}^{\frac{\gamma+1}{2(\gamma-1)}} \tag{C22}$$

$$\left(\frac{W_{cr}}{V_{cr}}\right)_3 = \left\{1 - \frac{\gamma - 1}{\gamma + 1}\left[\frac{2UV_{u,3}}{V_{cr,3}^2} - \left(\frac{U}{V_{cr,3}}\right)^2\right]\right\}^{1/2} \tag{C23}$$

$$\frac{p_3''}{p_3'} = \left\{1 - \frac{\gamma - 1}{\gamma + 1}\left[\frac{2UV_{u,3}}{V_{cr,3}^2} - \left(\frac{U}{V_{cr,3}}\right)^2\right]\right\}^{\frac{\gamma}{\gamma-1}} \tag{C24}$$

$$\left(\frac{W}{V_{cr}}\right)_3 = \left[\left(\frac{W_u}{V_{cr}}\right)_3^2 + \left(\frac{V_x}{V_{cr}}\right)_3^2\right]^{1/2} \tag{C25}$$

where

$$\left(\frac{W_u}{V_{cr}}\right)_3 = \left(\frac{V_u}{V_{cr}}\right)_3 - \frac{U}{V_{cr,3}}$$

$$\left(\frac{V_x}{V_{cr}}\right)_3 = \left(\frac{V}{V_{cr}}\right)_3 \cos \alpha_3$$

$$\left(\frac{V_u}{V_{cr}}\right)_3 = \left(\frac{V}{V_{cr}}\right)_3 \sin \alpha_3$$

and

$$\frac{U}{V_{cr,3}} = \left(\frac{U}{V_{cr,1}}\right)\left(\frac{V_{cr,1}}{V_{cr,2}}\right)$$

since $V_{cr,2} = V_{cr,3}$. The quantity $V_{cr,1}/V_{cr,2}$ can be obtained from equation (C10).

The outlet conditions are calculated by an iteration similar to the technique that was used for the first-stage rotor. This procedure assumes as a first approximation that $(\rho''W_{cr})_4 = (\rho''W_{cr})_3$, which in effect is assuming that $p''_4 = p''_3$, since $W_{cr,4} = W_{cr,3}$. Then, from continuity,

$$\left(\frac{\rho W}{\rho'' W_{cr}}\right)_4 = \left(\frac{\rho W}{\rho'' W_{cr}}\right)_3 \frac{\cos\beta_3}{\cos\beta_4}$$

where the flow angle β_3 is determined from $(W_u/V_{cr})_3$ and $(V_x/V_{cr})_3$, and the flow angle β_4 equals the blade angle, 44.6°. This approximate value of $(\rho W/\rho'' W_{cr})_4$ is used to solve the following equation for $(W/W_{cr})_4$:

$$\left(\frac{\rho W}{\rho'' W_{cr}}\right)_4 = \left(\frac{W}{W_{cr}}\right)_4 \left[1 - \frac{\gamma - 1}{\gamma + 1}\left(\frac{W}{W_{cr}}\right)_4^2\right]^{\frac{1}{\gamma-1}} \tag{C26}$$

The incidence angle is determined from the inlet flow angle and the blade angle

$$i_3 = 48.8^\circ - \beta_3$$

The total-pressure ratio across the blade row is determined from the following equation:

$$\frac{p''_4}{p''_3} = \left(1 - \frac{\frac{\gamma - 1}{\gamma + 1}\left\{2k\left[\left(\frac{W}{W_{cr}}\right)_3^2 + \left(\frac{W}{W_{cr}}\right)_4^2\right] + \sin^2 i_3\left(\frac{W}{W_{cr}}\right)_3^2\right\}}{1 - \frac{\gamma - 1}{\gamma + 1}\left(\frac{W}{W_{cr}}\right)_4^2}\right)^{\frac{\gamma}{\gamma-1}} \tag{C27}$$

The value of $(\rho W/\rho'' W_{cr})_4$ is corrected by dividing the approximated value by p_4''/p_3''. Equations (C26) and (C27) are resolved until the assumed value of $(\rho W/\rho'' W_{cr})_4$ is equal to the final value. The relative flow angle β_4 was taken equal to the blade angle up to the choking point. It was assumed that supercritical expansion could occur out of the second-stage rotor to the turbine limiting-loading point. The determination of the behavior of the flow angle β_4 was similar to that of equation (C21) except that all quantities had to be evaluated relative to the moving blade row. The limiting-loading point, defined as the point at which the local axial Mach number is 1, can be expressed in terms of critical-velocity ratio and flow angle as

$$\left(\frac{V}{V_{cr}}\right)_4 = \left(\frac{\frac{\gamma + 1}{2}}{\cos^2\alpha_4 + \frac{\gamma - 1}{2}}\right)^{1/2} \tag{C28}$$

Turbine-outlet conditions. - The work parameter for the second stage is given by

$$\frac{V_{cr,4}}{V_{cr,3}} = \left(1 - 2\,\frac{\gamma - 1}{\gamma + 1}\,\frac{U\,\Delta V_{u,3\text{-}4}}{V_{cr,3}^2}\right)^{1/2} \tag{C29}$$

where

$$\frac{\Delta V_{u,3\text{-}4}}{V_{cr,3}} = \frac{V_{u,3}}{V_{cr,3}} - \frac{V_{u,4}}{V_{cr,3}}$$

and

$$\frac{V_{u,4}}{V_{cr,3}} = \left(\frac{W}{W_{cr}}\right)_4 \sin\beta_4 \left(\frac{W_{cr}}{V_{cr}}\right)_3 - \frac{U}{V_{cr,3}}$$

The absolute to relative total-pressure ratio at the turbine outlet is given by

$$\frac{p_4'}{p_4''} = \left[1 - \frac{\gamma - 1}{\gamma + 1}\left(\frac{W_u}{W_{cr}}\right)_4^2 + \frac{\gamma - 1}{\gamma + 1}\left(\frac{V_u}{W_{cr}}\right)_4^2\right]^{\frac{\gamma}{\gamma-1}} \tag{C30}$$

where

$$\left(\frac{W_u}{W_{cr}}\right)_4 = \left(\frac{W}{W_{cr}}\right)_4 \sin \beta_4$$

and

$$\left(\frac{V_u}{W_{cr}}\right)_4 = \left(\frac{W_u}{W_{cr}}\right)_4 - \frac{U}{W_{cr,4}} = \left(\frac{W_u}{W_{cr}}\right)_4 - \frac{U}{V_{cr,3}}\left(\frac{V_{cr}}{W_{cr}}\right)_3$$

The static- to total-pressure ratio at the turbine outlet is obtained from

$$\frac{p_4}{p_4'} = \left\{1 - \frac{\gamma - 1}{\gamma + 1}\left[\left(\frac{V_u}{V_{cr}}\right)_4^2 + \left(\frac{V_x}{V_{cr}}\right)_4^2\right]\right\}^{\frac{\gamma}{\gamma-1}} \tag{C31}$$

where

$$\left(\frac{V_u}{V_{cr}}\right)_4 = \left(\frac{V_{u,4}}{V_{cr,3}}\right)\left(\frac{V_{cr,3}}{V_{cr,4}}\right)$$

and

$$\left(\frac{V_x}{V_{cr}}\right)_4 = \left(\frac{W}{W_{cr}}\right)_4 \cos \beta_4\left(\frac{W_{cr}}{V_{cr}}\right)_3 \frac{V_{cr,3}}{V_{cr,4}}$$

The overall turbine pressure ratio is then

$$\frac{p_4}{p_0'} = \left(\frac{p_2'}{p_0'}\right)\left(\frac{p_3'}{p_2'}\right)\left(\frac{p_3''}{p_3'}\right)\left(\frac{p_4''}{p_3''}\right)\left(\frac{p_4'}{p_4''}\right)\left(\frac{p_4}{p_4'}\right) \tag{C32}$$

The turbine efficiency is obtained from

$$\eta_s = \frac{1 - \left(\frac{V_{cr,2}}{V_{cr,1}}\right)^2 \left(\frac{V_{cr,4}}{V_{cr,3}}\right)^2}{1 - \left(\frac{p_4}{p_0'}\right)^{\frac{\gamma-1}{\gamma}}} \tag{C33}$$

The turbine blade- to jet-speed ratio ν is calculated by using equation (1).

$$\nu = \frac{\frac{U}{V_{cr,0}}}{\left\{\frac{\gamma + 1}{\gamma - 1}\left[1 - \left(\frac{p_4}{p_0'}\right)^{\frac{\gamma-1}{\gamma}}\right]\right\}^{1/2}} \tag{1}$$

The turbine equivalent specific work was calculated from the following equation:

$$\frac{\Delta h'}{\theta_{cr}} = \left[1 - \left(\frac{V_{cr,2}}{V_{cr,1}}\right)^2 \left(\frac{V_{cr,4}}{V_{cr,3}}\right)^2\right] \frac{V_{cr,ref}^2}{2gJ\left(\frac{\gamma - 1}{\gamma + 1}\right)} \tag{C34}$$

Thus, all of the quantities that are required to show the performance characteristics are evaluated.

REFERENCES

1. Wong, Robert Y., and Darmstadt, David L.: Comparison of Experimentally Obtained Performance of Two Single-Stage Turbines with Design Ratios of Blade to Jet Speed of 0.191 and 0.262 Operated in Hydrogen and Nitrogen. NASA TM X-415, 1961.

2. Rohlik, Harold E.: Investigation of Eight-Stage Bleed-Type Turbine for Hydrogen-Propelled Nuclear Rocket Applications. I - Design of Turbine and Experimental Performance of First Two Stages. NASA TM X-475, 1961.

3. Stewart, Warner L.: Analytical Investigation of Multistage-Turbine Efficiency Characteristics in Terms of Work and Speed Requirements. NACA RM E57K22b, 1958.

4. Stewart, Warner L., and Evans, David G.: Analytical Study of Losses at Off-Design Conditions for a Fixed-Geometry Turbine. NACA RM E53K06, 1954.

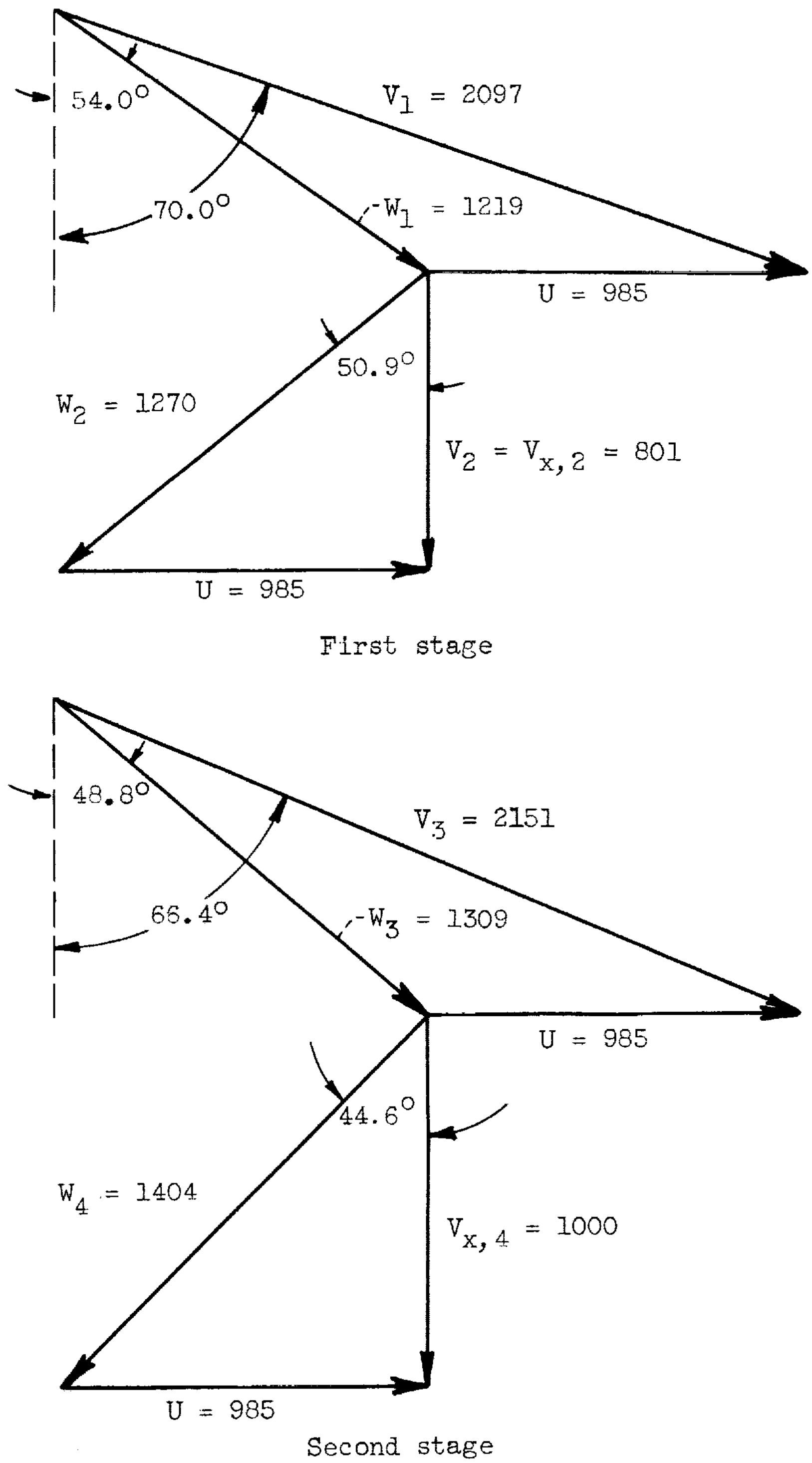

Figure 1. - Velocity diagram of two-stage impulse turbine used as model for analysis. (All velocities are in feet per second.)

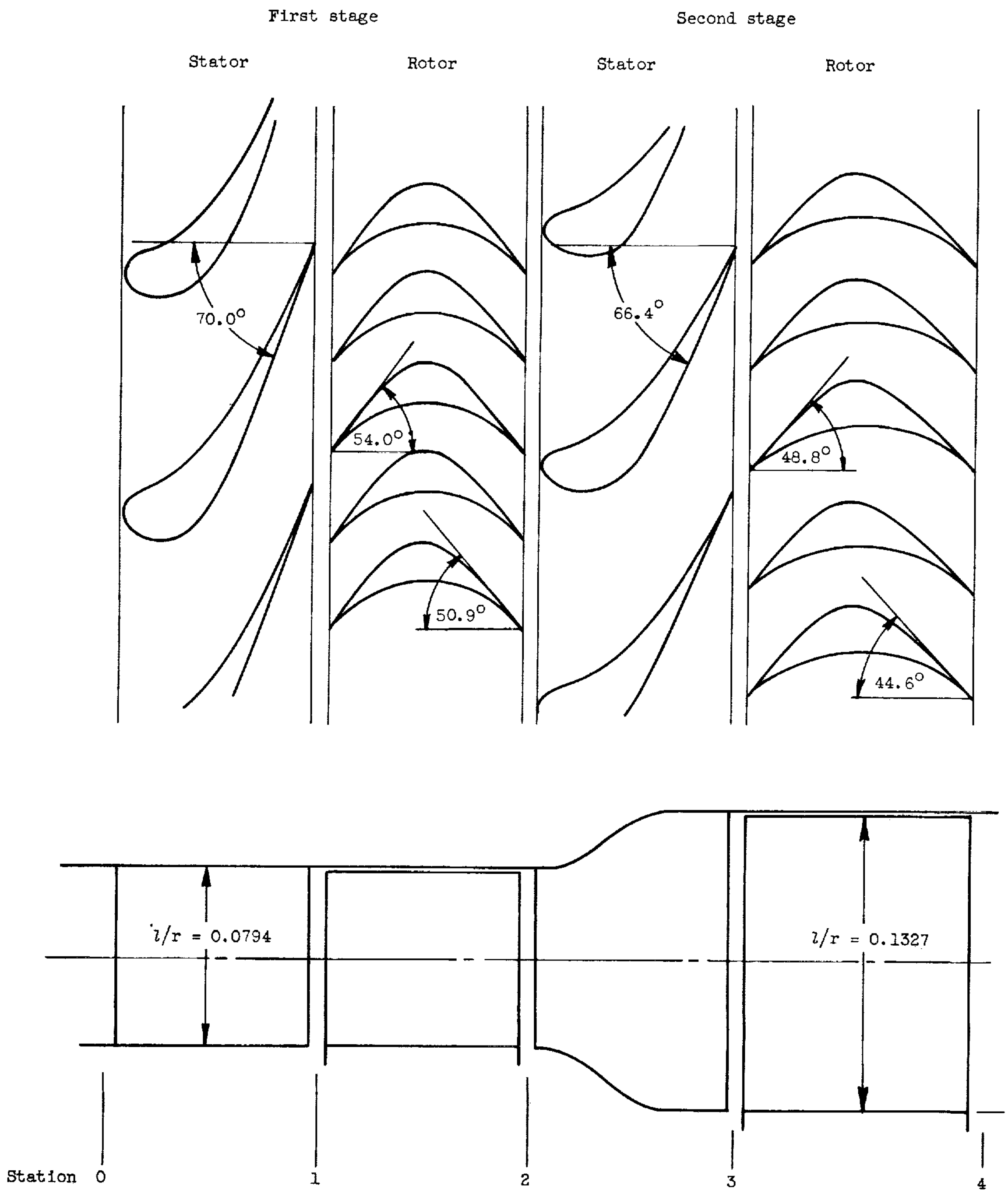

Figure 2. - Turbine geometric characteristics used as model in analysis.

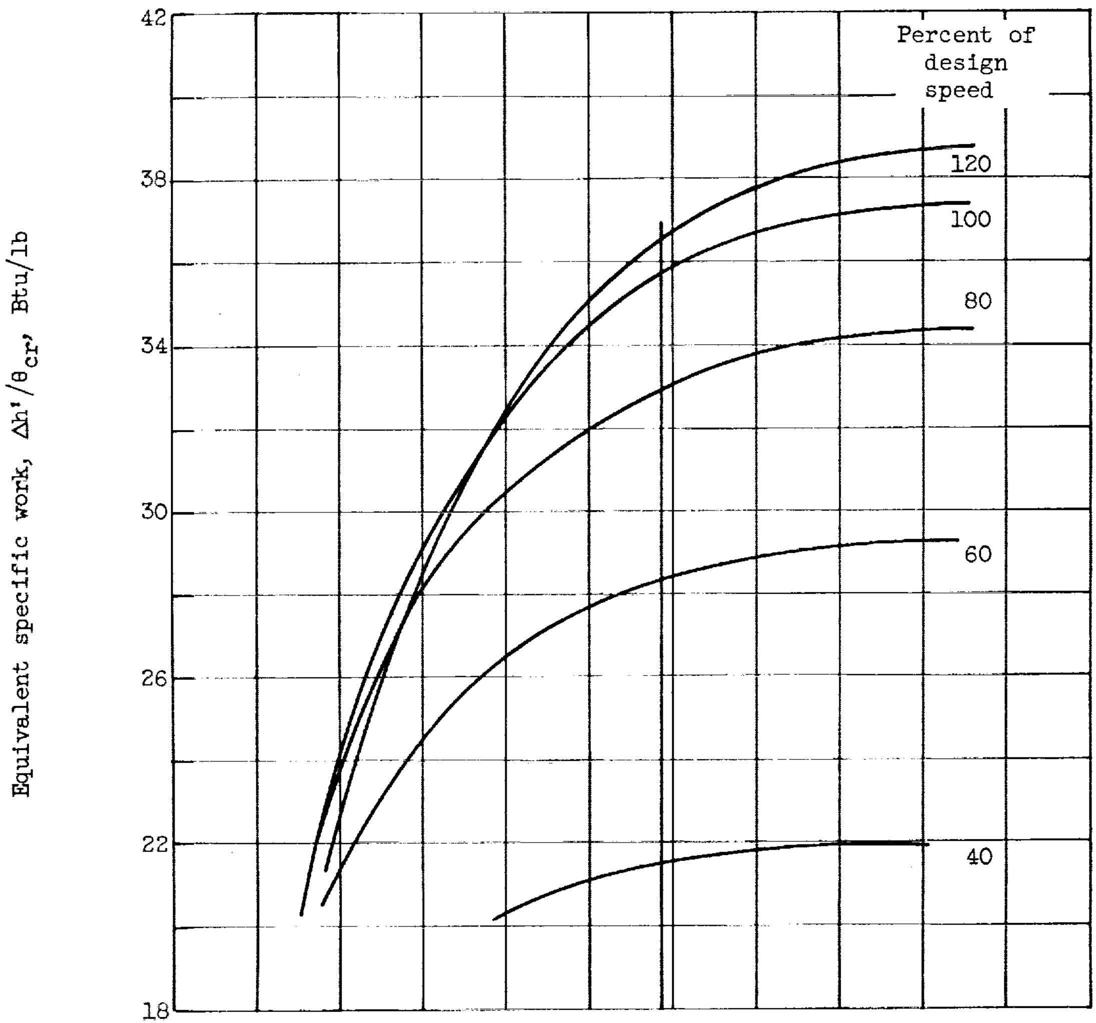

(a) Work.

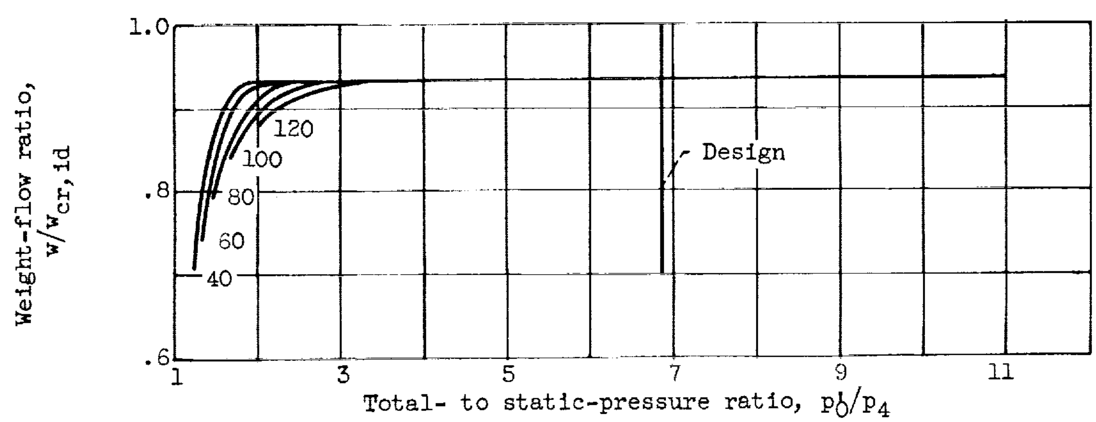

(b) Weight flow.

Figure 3. - Turbine performance. Ratio of specific heats, 1.53.

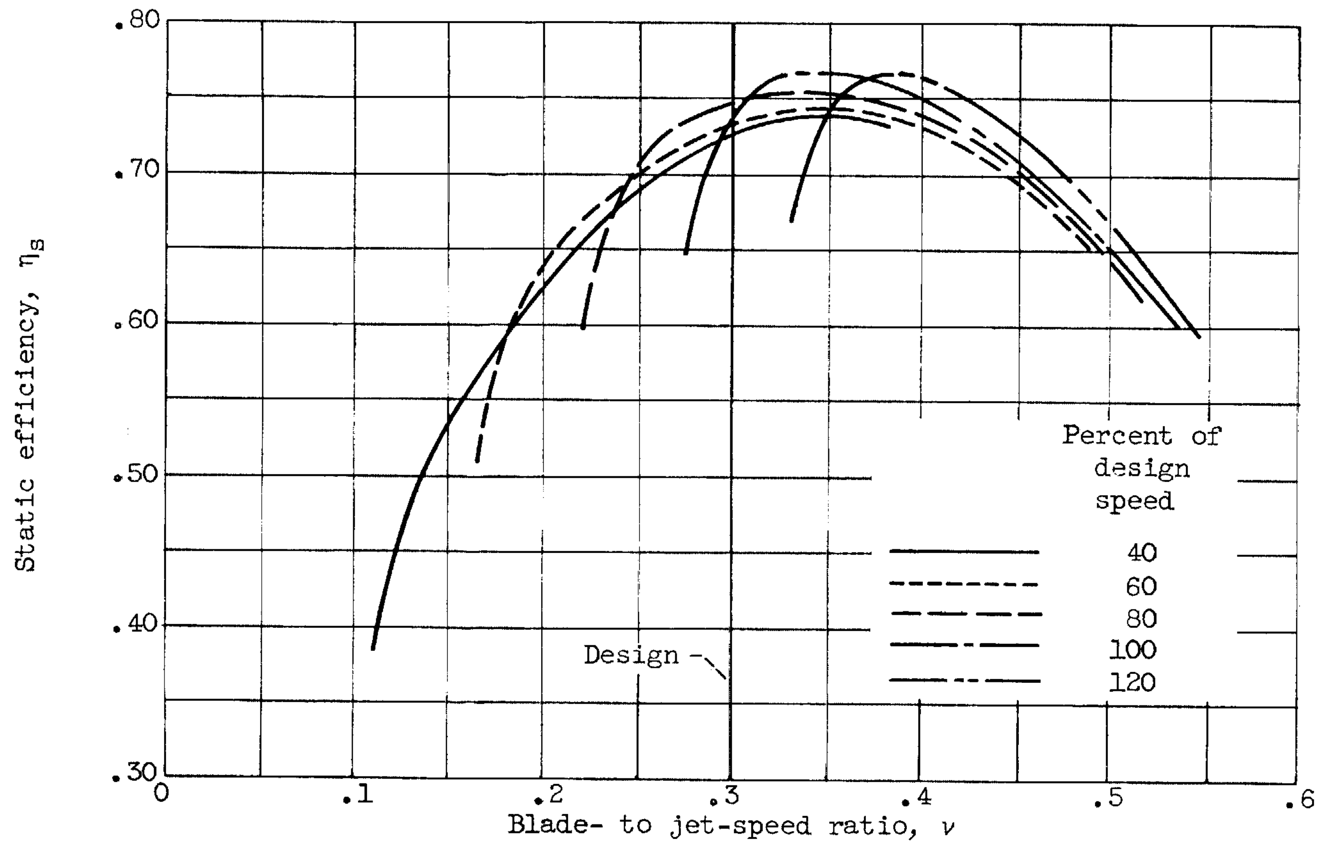

Figure 4. - Turbine-efficiency characteristics. Ratio of specific heats, 1.53.

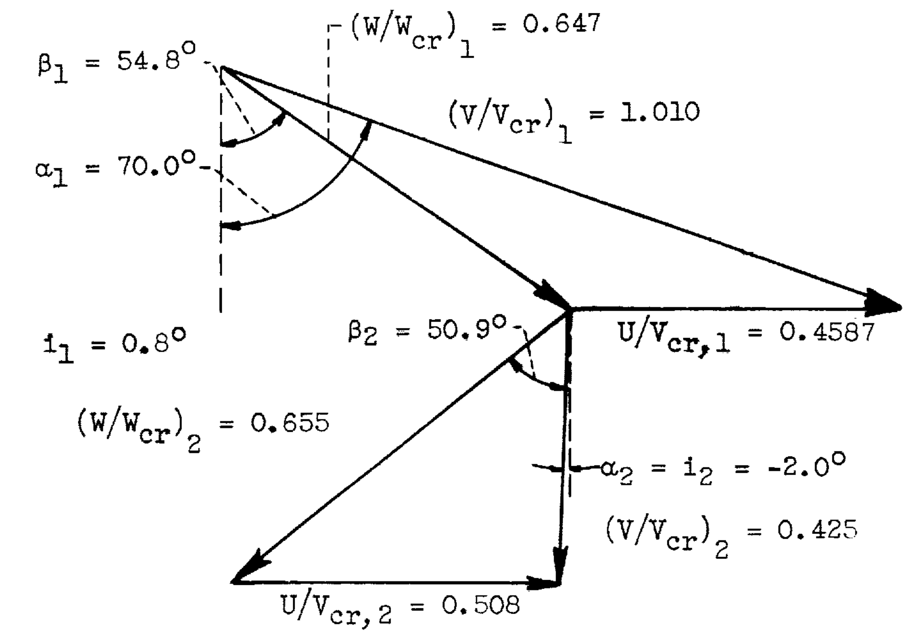

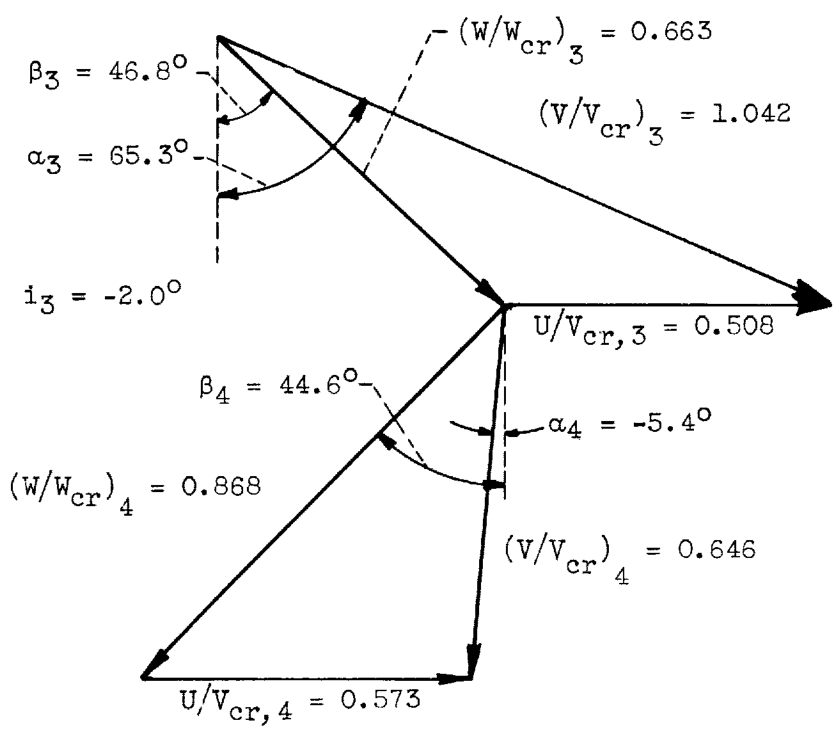

Figure 5. - Turbine velocity diagrams obtained at design point. Ratio of specific heats, 1.53.

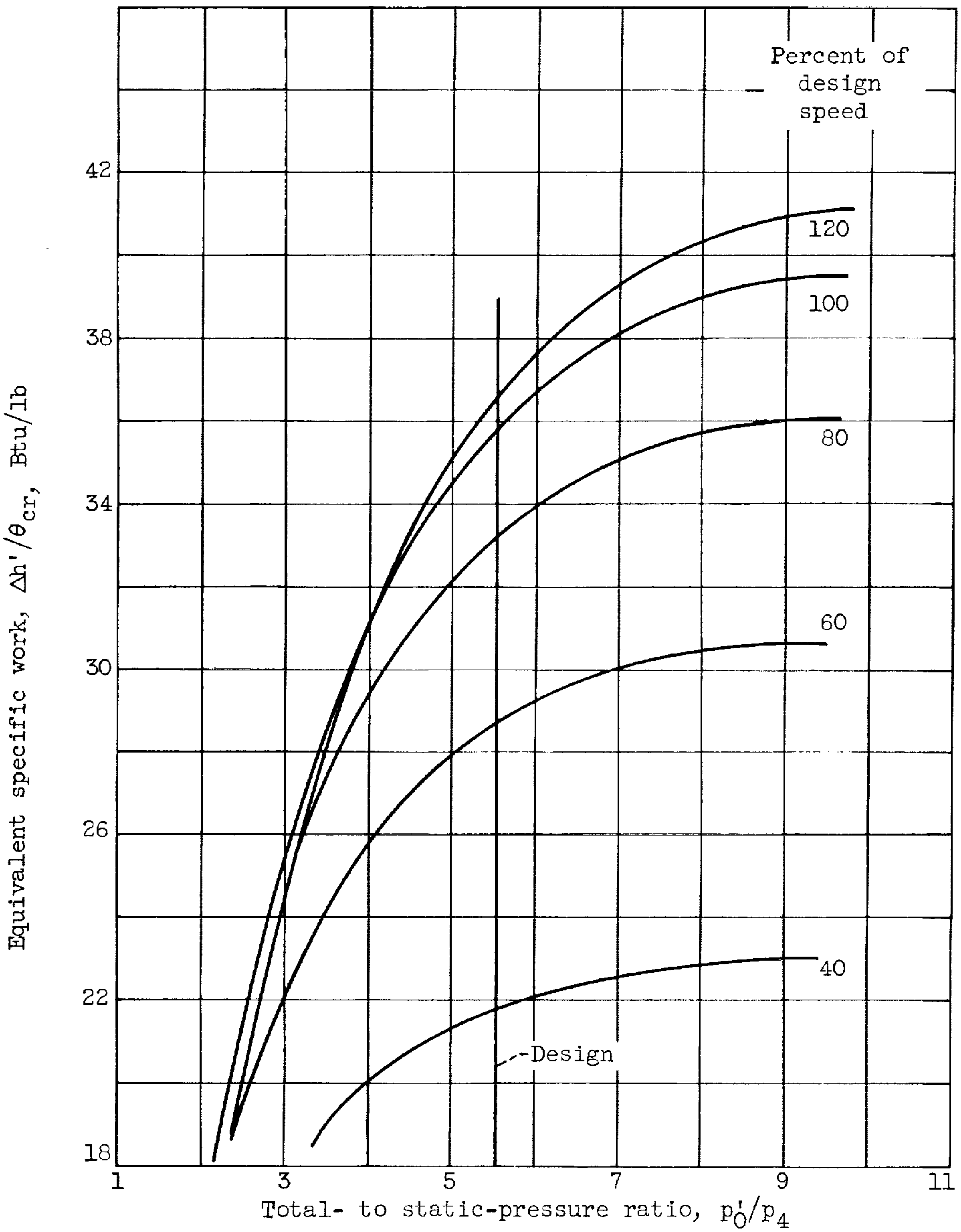

Figure 6. - Turbine performance. Ratio of specific heats, 1.4.

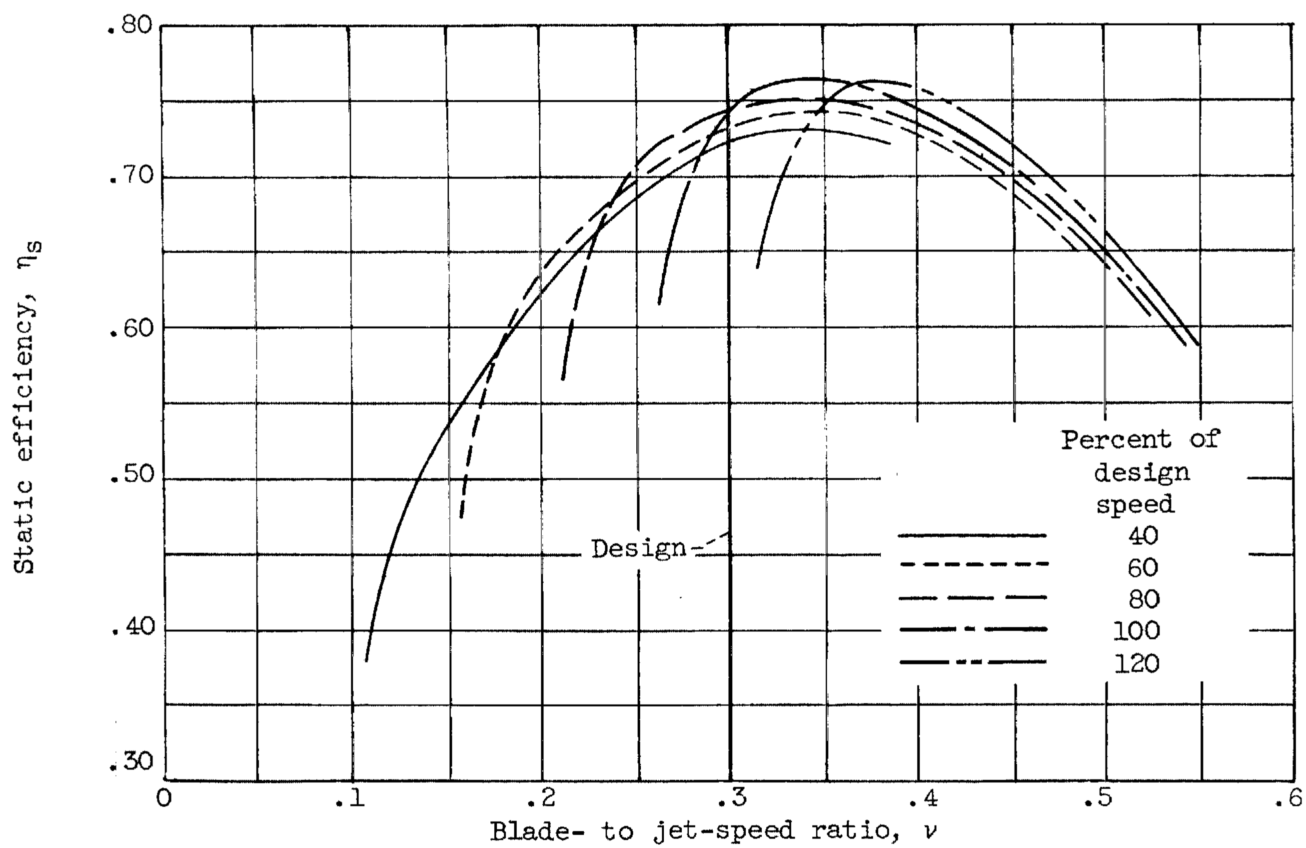

Figure 7. - Turbine-efficiency characteristics. Ratio of specific heats, 1.4.

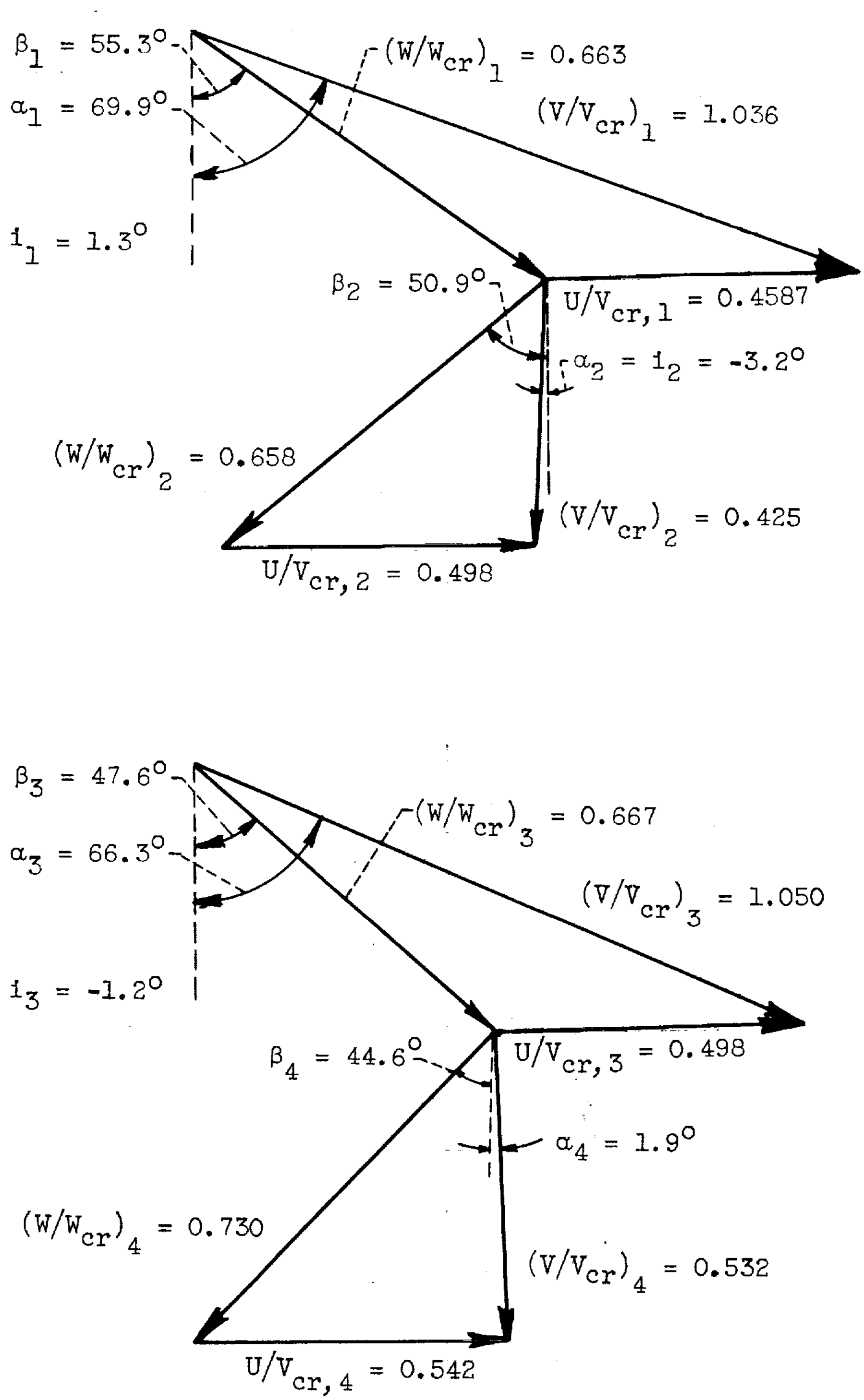

Figure 8. - Turbine velocity diagrams obtained at design point. Ratio of specific heats, 1.4.

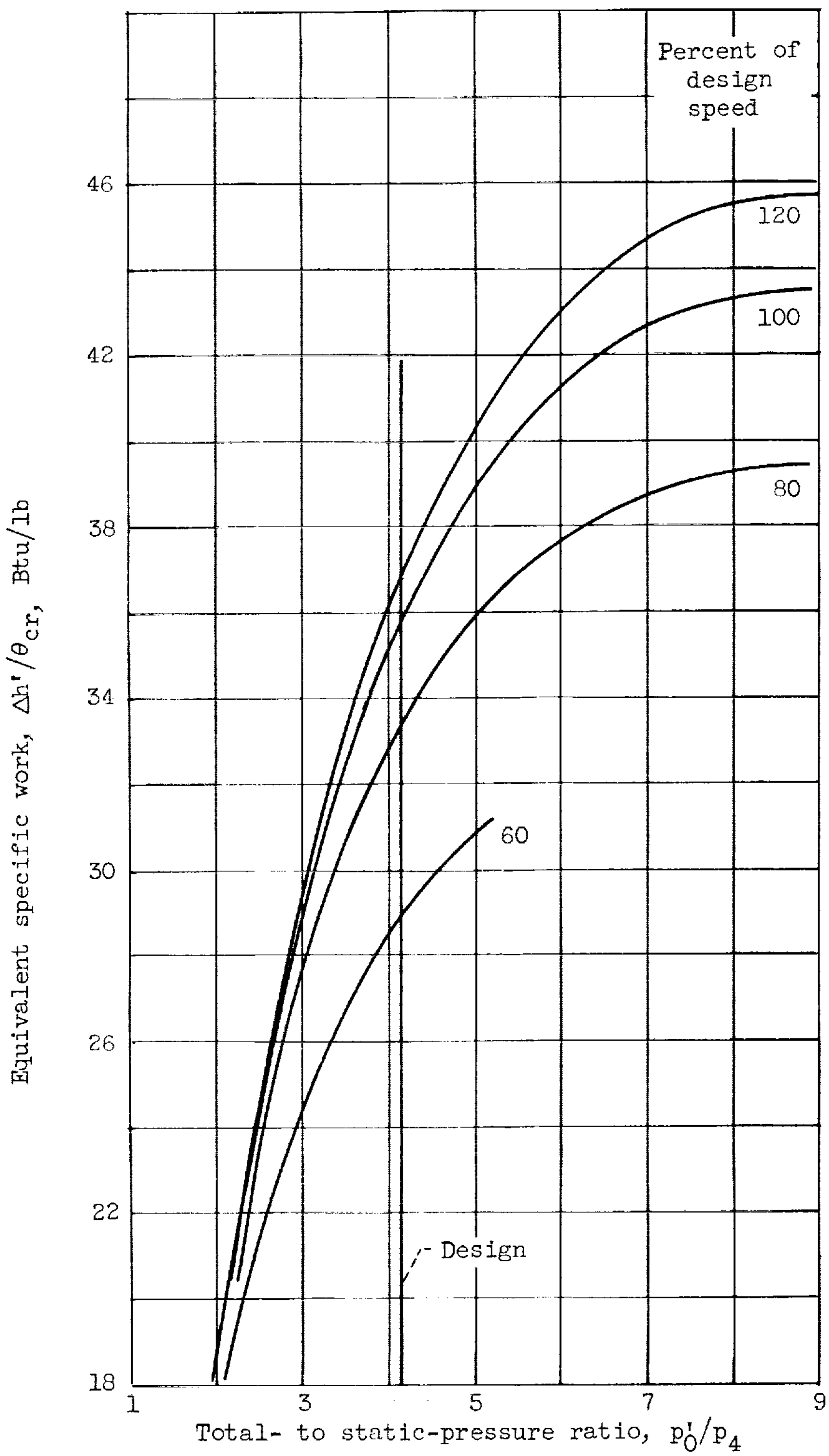

Figure 9. - Turbine performance. Ratio of specific heats, 1.2.

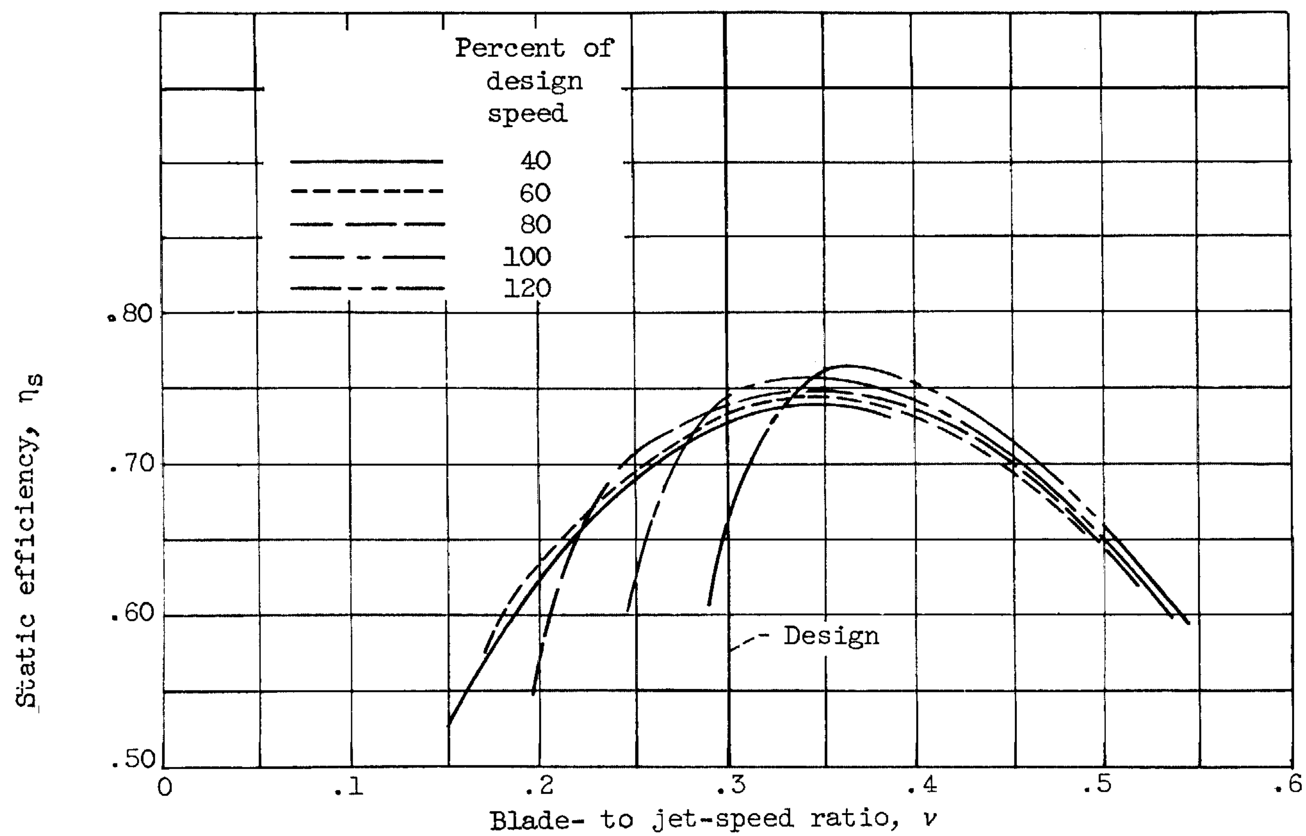

Figure 10. - Turbine-efficiency characteristics. Ratio of specific heats, 1.2.

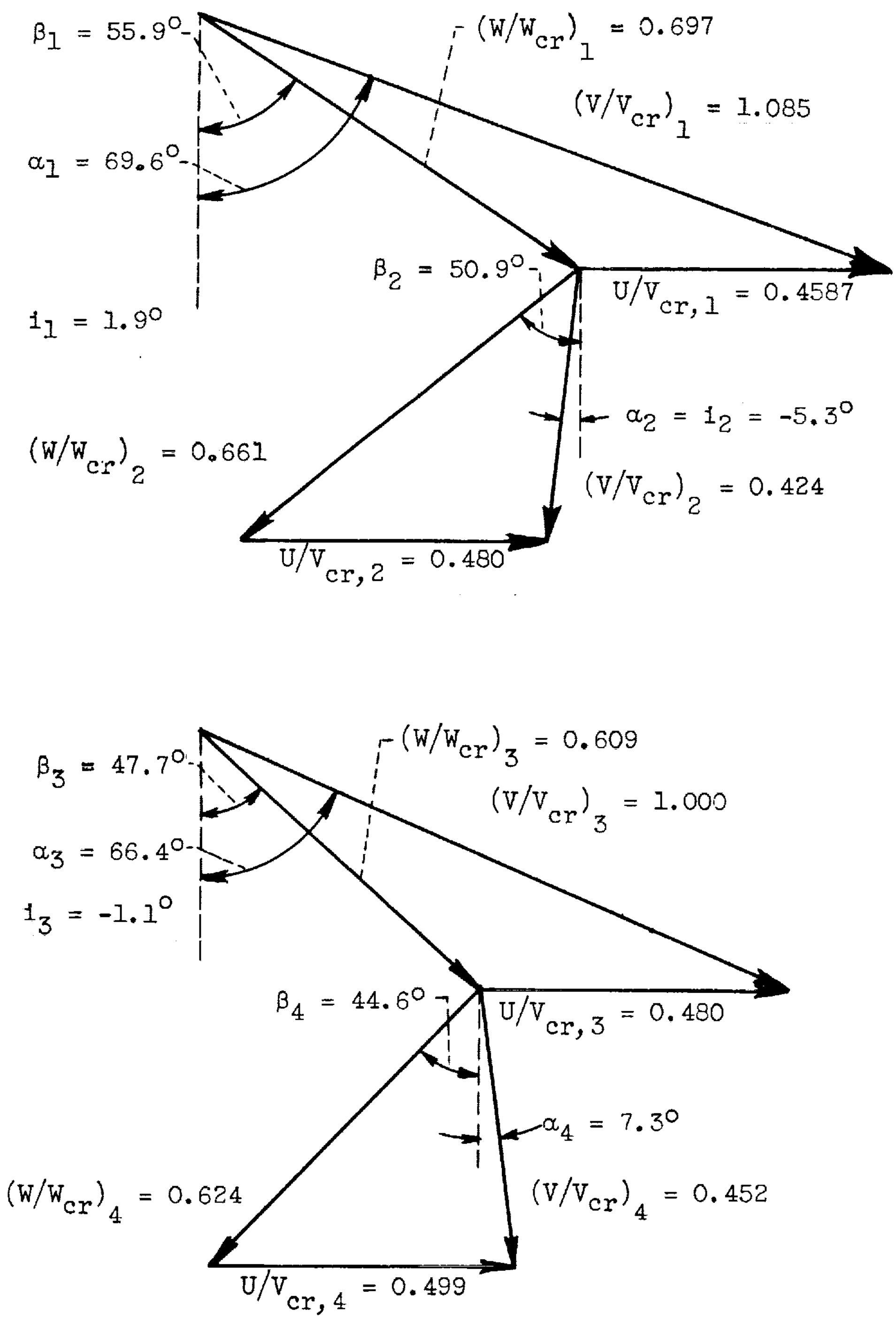

Figure 11. - Turbine velocity diagrams obtained at design point. Ratio of specific heats, 1.2.

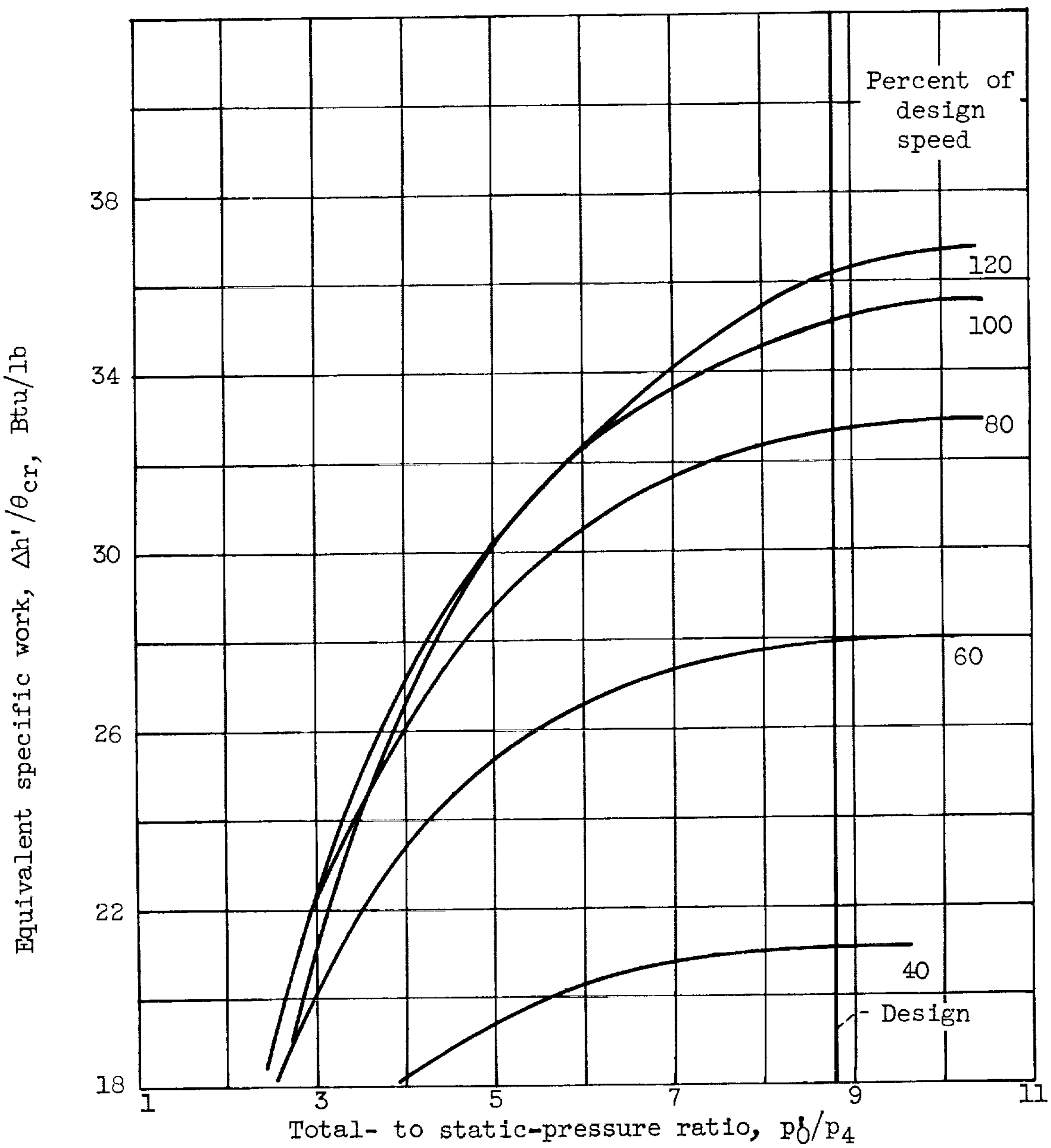

Figure 12. - Turbine performance. Ratio of specific heats, $1\frac{2}{3}$.

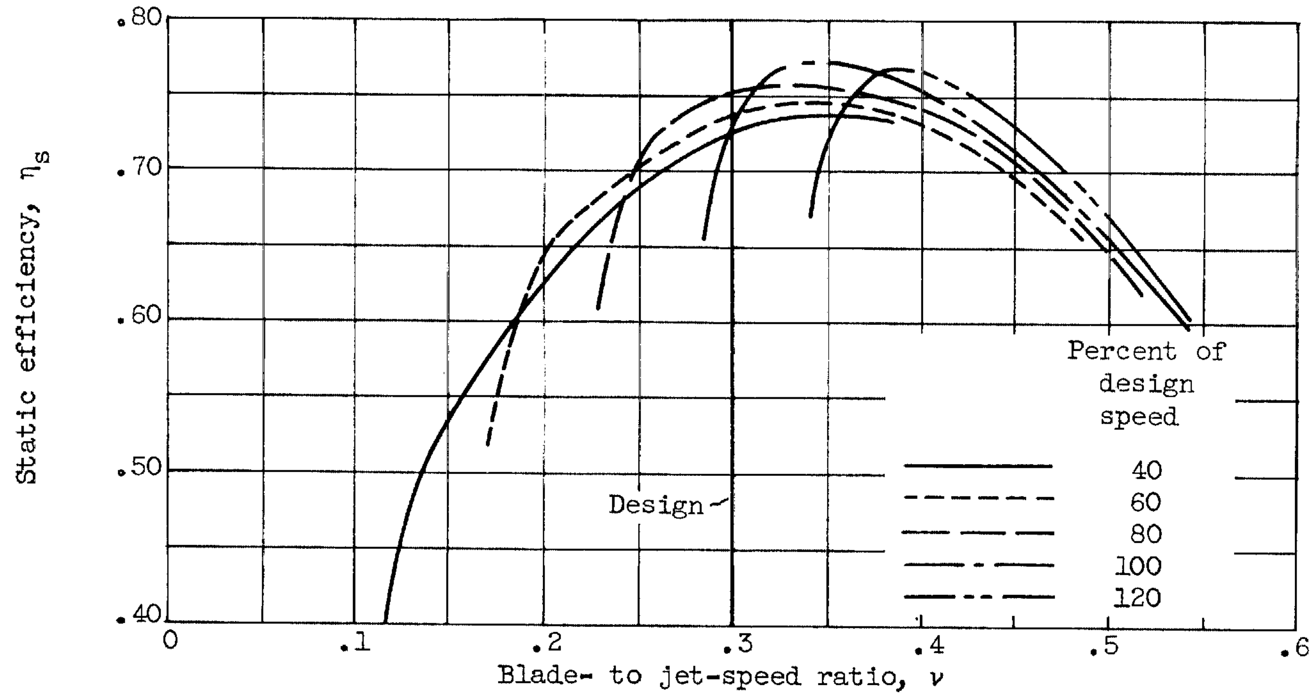

Figure 13. - Turbine-efficiency characteristics. Ratio of specific heats, $1\frac{2}{3}$.

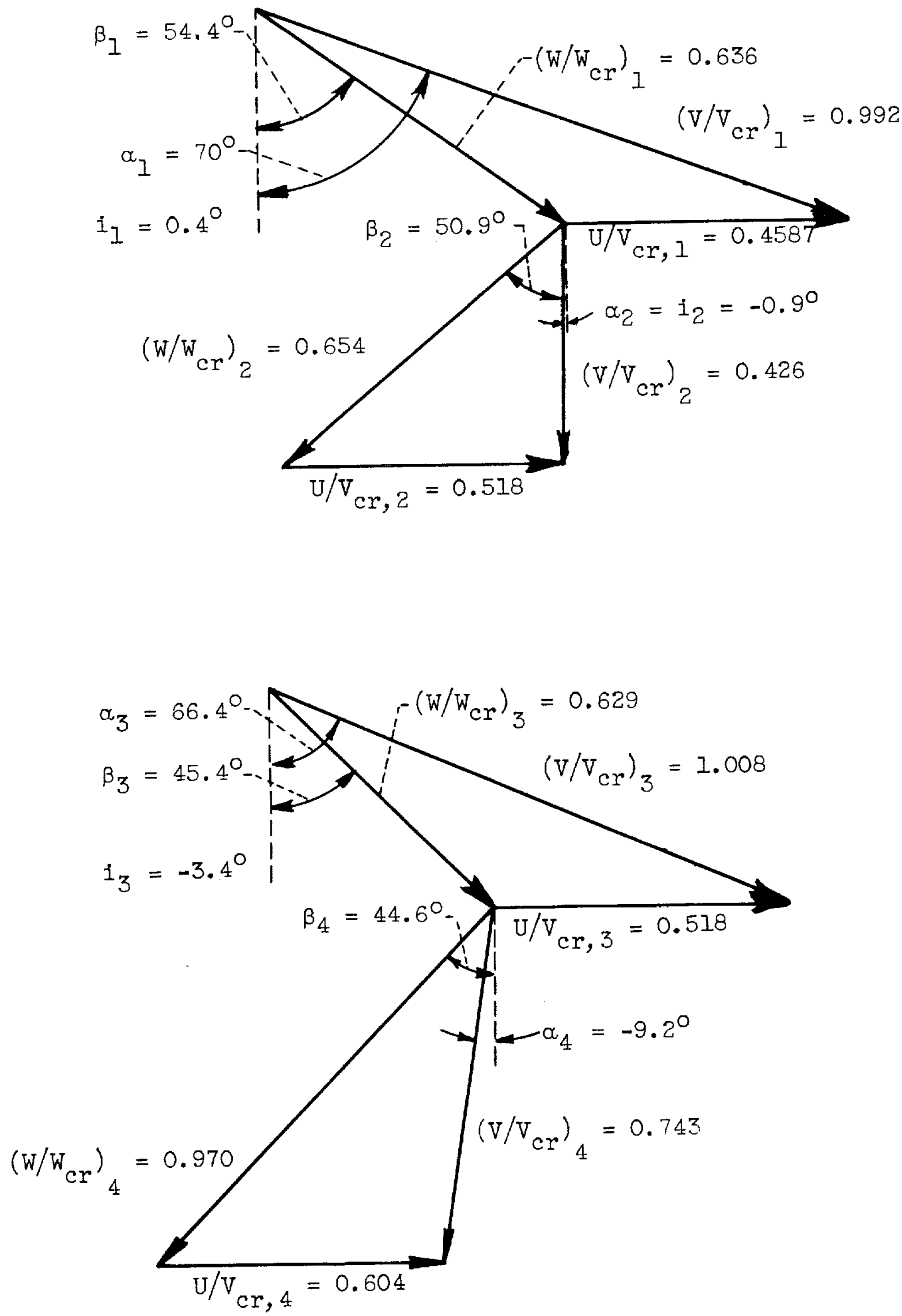

Figure 14. - Turbine velocity diagrams obtained at design point. Ratio of specific heats, $1\frac{2}{3}$.

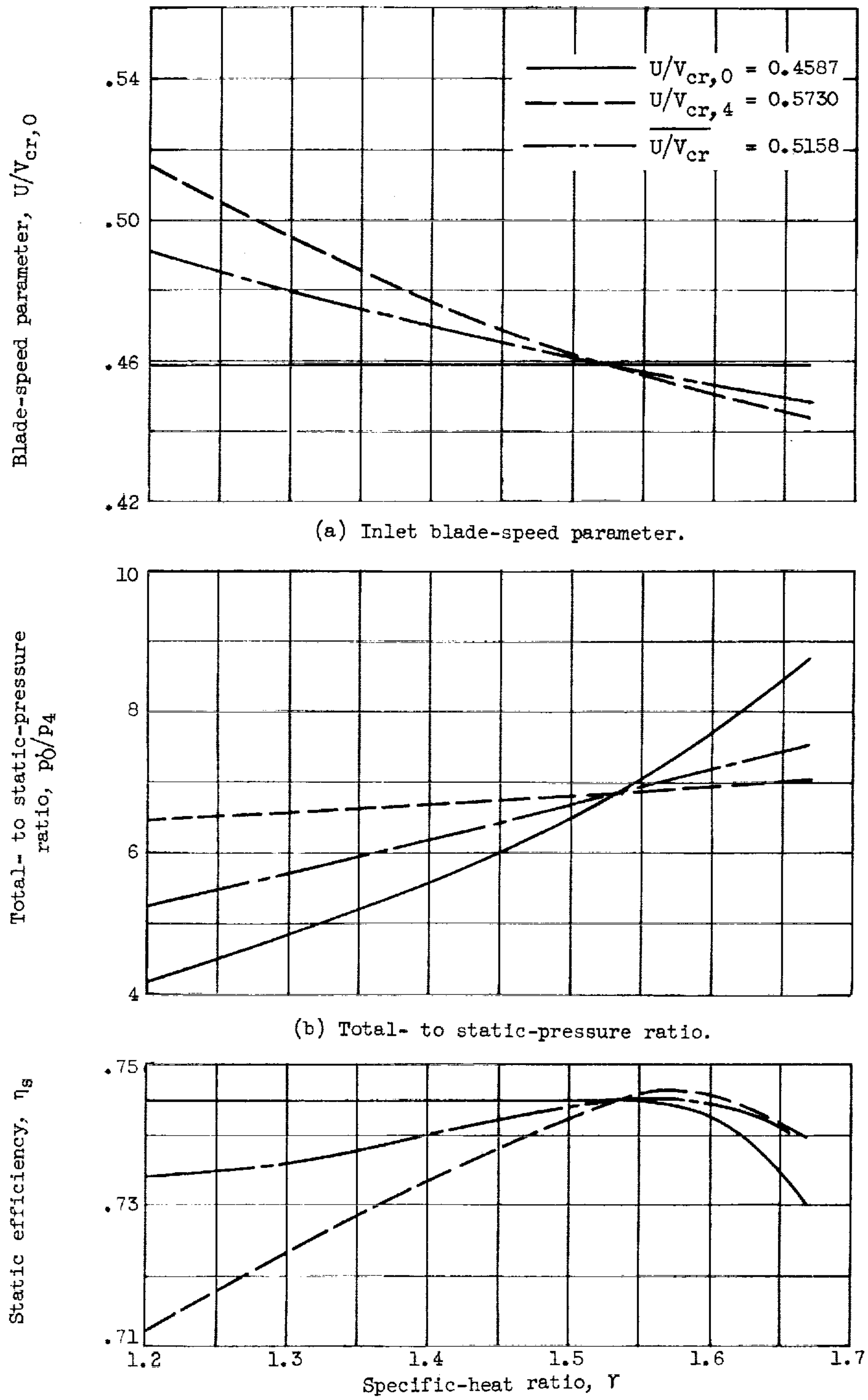

(c) Static efficiency.

Figure 15. - Variation of inlet blade-speed parameter, total- to static-pressure ratio, and static efficiency with specific-heat ratio for three types of specified blade-speed parameter.

NASA TN D-1288
National Aeronautics and Space Administration.
ANALYTICAL INVESTIGATION OF PERFORMANCE OF TWO-STAGE TURBINE OVER A RANGE OF RATIOS OF SPECIFIC HEATS FROM 1.2 TO 1-2/3. Warren J. Whitney and Warner L. Stewart. July 1962. 46p. OTS price, $1.25.
(NASA TECHNICAL NOTE D-1288)

Turbine performance was only slightly affected by the variation in the specific-heat ratio except when the turbine was operated near limiting loading. For operation near limiting loading the best blade-speed parameter for estimating turbine performance was the ratio of blade speed to the average of the turbine-inlet and -outlet critical velocities.

I. Whitney, Warren J.
II. Stewart, Warner L.
III. NASA TN D-1288

(Initial NASA distribution: 2, Aerodynamics, missiles and space vehicles; 38, Propulsion systems, air-jet; 39, Propulsion systems, liquid-fuel rockets; 41, Propulsion systems, electric.)

NASA

NASA TN D-1288
National Aeronautics and Space Administration.
ANALYTICAL INVESTIGATION OF PERFORMANCE OF TWO-STAGE TURBINE OVER A RANGE OF RATIOS OF SPECIFIC HEATS FROM 1.2 TO 1-2/3. Warren J. Whitney and Warner L. Stewart. July 1962. 46p. OTS price, $1.25.
(NASA TECHNICAL NOTE D-1288)

Turbine performance was only slightly affected by the variation in the specific-heat ratio except when the turbine was operated near limiting loading. For operation near limiting loading the best blade-speed parameter for estimating turbine performance was the ratio of blade speed to the average of the turbine-inlet and -outlet critical velocities.

I. Whitney, Warren J.
II. Stewart, Warner L.
III. NASA TN D-1288

(Initial NASA distribution: 2, Aerodynamics, missiles and space vehicles; 38, Propulsion systems, air-jet; 39, Propulsion systems, liquid-fuel rockets; 41, Propulsion systems, electric.)

NASA

NASA TN D-1288
National Aeronautics and Space Administration.
ANALYTICAL INVESTIGATION OF PERFORMANCE OF TWO-STAGE TURBINE OVER A RANGE OF RATIOS OF SPECIFIC HEATS FROM 1.2 TO 1-2/3. Warren J. Whitney and Warner L. Stewart. July 1962. 46p. OTS price, $1.25.
(NASA TECHNICAL NOTE D-1288)

Turbine performance was only slightly affected by the variation in the specific-heat ratio except when the turbine was operated near limiting loading. For operation near limiting loading the best blade-speed parameter for estimating turbine performance was the ratio of blade speed to the average of the turbine-inlet and -outlet critical velocities.

I. Whitney, Warren J.
II. Stewart, Warner L.
III. NASA TN D-1288

(Initial NASA distribution: 2, Aerodynamics, missiles and space vehicles; 38, Propulsion systems, air-jet; 39, Propulsion systems, liquid-fuel rockets; 41, Propulsion systems, electric.)

NASA

NASA TN D-1288
National Aeronautics and Space Administration.
ANALYTICAL INVESTIGATION OF PERFORMANCE OF TWO-STAGE TURBINE OVER A RANGE OF RATIOS OF SPECIFIC HEATS FROM 1.2 TO 1-2/3. Warren J. Whitney and Warner L. Stewart. July 1962. 46p. OTS price, $1.25.
(NASA TECHNICAL NOTE D-1288)

Turbine performance was only slightly affected by the variation in the specific-heat ratio except when the turbine was operated near limiting loading. For operation near limiting loading the best blade-speed parameter for estimating turbine performance was the ratio of blade speed to the average of the turbine-inlet and -outlet critical velocities.

I. Whitney, Warren J.
II. Stewart, Warner L.
III. NASA TN D-1288

(Initial NASA distribution: 2, Aerodynamics, missiles and space vehicles; 38, Propulsion systems, air-jet; 39, Propulsion systems, liquid-fuel rockets; 41, Propulsion systems, electric.)

NASA